INFORMATION TO USERS

This manuscript has been reproduced from the microfilm master. UMI films the text directly from the original or copy submitted. Thus, some thesis and dissertation copies are in typewriter face, while others may be from any type of computer printer.

The quality of this reproduction is dependent upon the quality of the copy submitted. Broken or indistinct print, colored or poor quality illustrations and photographs, print bleedthrough, substandard margins, and improper alignment can adversely affect reproduction.

In the unlikely event that the author did not send UMI a complete manuscript and there are missing pages, these will be noted. Also, if unauthorized copyright material had to be removed, a note will indicate the deletion.

Oversize materials (e.g., maps, drawings, charts) are reproduced by sectioning the original, beginning at the upper left-hand corner and continuing from left to right in equal sections with small overlaps.

ProQuest Information and Learning
300 North Zeeb Road, Ann Arbor, MI 48106-1346 USA
800-521-0600

Composite Broad-Band Fiber Raman Amplifiers Using Incoherent Pumping

Bing Han

A Thesis

In

The Department

of

Electrical and Computer Engineering

Presented in Partial Fulfillment of the Requirements

for the Degree of Master of Applied Science (Electrical and Computer Engineering) at

Concordia University

Montreal, Quebec, Canada

March 2005

Abstract

Composite Broad-Band Fiber Raman Amplifiers

Using Incoherent Pumping

Bing Han

Use of novel incoherent pump source to dual-stage fiber Raman amplifiers (FRA's)--dispersion compensated fiber Raman amplifier (DCRA) is investigated and the performance is compared to results with the conventional coherent pumping for the first time. To achieve accurate modeling, a theoretical model of FRA's, which includes effects of multiple-path interference (MPI), anti-Stokes, and Rayleigh scattering, is used. Modeling of the incoherent pump is also given theoretically. This model is tested to be accurate.

Investigations are based on above models of DCRA with one and two incoherent pumps. By comparing the performances of DCRA with coherent pumps, we concluded that better gain and noise performance can be achieved using less incoherent pumps than coherent pumps.

Also, gain flatness and OSNR flatness of the dual-stage fiber Raman amplifiers are investigated separately and simultaneously, using one and two incoherent pumps. Optimum parameters of the incoherent pump such as center wavelength, FWHM (full width at half maximum) and pump power are found for signal bandwidths up to 100 nm. It is shown that in this combined configuration, there is a trade-off in obtaining the flatness of gain and OSNR. But with a suitable pumping scheme, both gain and OSNR flatness can be achieved simultaneously.

Acknowledgements

I would like to express my gratitude to my supervisor, professor John Xiupu Zhang of Concordia University, for his essential guidance, inspiration, encouragement, suggestions, and openly sharing his knowledge and experience. I also want to give thanks to Dr. Peter Borg Gaarde of *OFS*® Company for his data and valuable information; and Dr. Xiang Zhou of *AT&T*® LABS-Research for his suggestions and opinions. In addition, I would like to thank my partners, Mm. Ting Zhang and Mm. Jinghong Fan for all the discussion and help during the construction of the thesis.

I would like to thank the Natural Science of Engineering Research Council of Canada and the Faculty of Electrical and Computer Engineering at Concordia University for supporting this project.

Finally, I would like to thank my family for their warm encouragement and support to complete the work.

Bing Han

Concordia University

February 2005

Contents

LIST OF FIGURES

LIST OF TABLES

Chapter 1

Introduction

This chapter will provide a clear picture of the background, origin, and targets of this thesis. First, three types of optical amplifiers are introduced in Section 1.1, including their brief histories, functions, and developments. The origination of this project is then given in Section 1.2, in which you can also find the basic idea of this work. Finally, Section 1.3 describes the structure of the thesis to help the reader understand this work.

1.1 Optical fiber amplifier

Used in fiber telecommunication systems, optical amplifiers are a great revolution since they avoid the complexity of O-E-O conversion, reduce the equipment cost, and extend the transmission span of the Wavelength Division Multiplexing (WDM) systems simultaneously. Erbium Doped Fiber Amplifier (EDFA), as the outstanding representative of optical amplifiers, has been widely used as the optical amplifier for the past 20 years thanks to its several advantages, such as high pumping and gain efficiency (without using high pump power, a 30 dB gain is easily attainable with a few miliWatts of pumping at 980 nm), low coupling loss to the transmission fiber, very low dependence of gain on light polarization, slow gain

dynamics, and immunity from interference effects (such as crosstalk and inter-modulation distortion) between different optical channels. But EDFA also has its drawbacks. In a doped fiber amplifier, the operating wavelength and the gain bandwidth are determined by the dopants rather than by the silica fiber. So EDFA can only be operated in the C-band (from 1525 to 1565 nm), and L-band (with the help of other mechanism). Fiber Raman amplifier, however, has many advantages over the EDFA. For instance, given the appropriate pumps, Raman gain can be produced at any wavelengths. So Raman gain not only exists in C- and L- band, but also exists in 1300 nm band, 1400 nm band, S- band, etc. And what's more, the Raman gain medium can be the transmission fiber itself, because Raman gain can exist wherever there is a fiber. For these reasons, the Raman amplifier is becoming more and more popular in long-haul and ultra-long haul WDM systems [3].

Conventional broad-band Raman amplifiers achieve wide gain bandwidth and flatness by multiplexing a set of pumps at fixed wavelengths with constant output powers. ±0.5 dB gain variation was obtained by multiplexing 12 pumps with a total power of 2.2 W, in a lab environment [24]. However, some questions still exist. On one hand, this approach needs high power pump diodes; too many pumps complicate the task; it is inconvenient to realize both in a lab and on site, so it will increase the application complexity and cost. On another hand, unwanted interactions between the continuous-wave pumps can cause impairments such as pump-pump Four Wave Mixing (FWM) and OSNR tilt. And what's more, it still needs to be confirmed whether the complicated structure and big power could cause other potential

nonlinearity defects. Recently, new pumping approaches have been developed to pursue a smaller gain tilt. In one approach, pumps at fixed wavelengths are time-division-multiplexed (TDM) so that only one pump, or a subset of pumps, is on at any given time. Another approach uses a single pump that is rapidly and repeatedly swept over the necessary wavelength range to achieve broad-band gain. An added benefit of this approach is that significantly lower gain ripple can be achieved because the gain spectrum is not constrained by using a fixed, predetermined number of pump wavelengths [35].

However, these approaches are only good to apply to the backward pumping scheme. Furthermore, cost-effective pump technologies have not been developed for these approaches so far. Therefore, it remains to be seen whether the performance advantages that can be gained by time-dependent Raman pumping are worth the additional cost and complexity.

Very recently distributed Raman amplifiers using incoherent pumps have been demonstrated to obtain a flat broadband gain [15]. The incoherent pump has a broader pump spectrum, very low relative intensity noise (RINs<-140 dB/Hz), and lower emission power. In contrast to the conventional coherent pumping source, the pumping power of the incoherent pumping source spreads over a wide wavelength range from several nanometers to tens of nanometers; the phase and polarization of incoherent pumping source are completely random. Thus, the Stimulated Brillouin impairment can be completely suppressed from incoherent pumping. Due to the random phase of incoherent pumps, the FWM generated by pump-pump, pump-ASE

noise and pump-signal is significantly reduced. Another benefit of using incoherent pumping is that the polarization multiplexer for the pumping source can be eliminated due to the random polarization of the pumping source. For distributed Raman amplifier with incoherent pumping, the signal amplification by Raman gain is given by the summation effect from pump power at the whole pump wavelength range.

Discrete Raman amplifier refers to a lumped element that is inserted into the transmission line, either to provide additional gain, or to compensate loss from other passive elements. Dispersion compensating fiber was invented originally to compensate the fiber dispersion and/or dispersion slope in the transmission fiber. However, it was found out that DCF is an excellent gain medium for discrete Raman amplifiers. Because the discrete Raman amplification only requires few kilometers of fiber; in addition, the small effective area and high *Ge* concentration of DCF provide high Raman gain efficiency. What's more, the DCF as a discrete Raman amplifier can give additional flexibility in the system; it can save more space in the practical application; and it is potentially low cost! For these reasons, Dispersion Compensated Raman Amplifier (DCRA) is becoming more and more widely used in the long-haul and ultra-long haul transmission system [48].

A *new design method* was demonstrated in [16] by moving part of the gain of long wavelength signals from the distributed Raman amplifier to the following discrete Raman amplifier to improve the total noise performance of the dual-stage fiber Raman amplifiers. In this paper, we apply the incoherent pump source to the two-stage amplifier—distributed Raman amplifier followed by a DCF as discrete

Raman amplifier, by adoption of the *New Design Method*, in order to find ways to obtain both gain and OSNR flatness, so as to improve the output stability and system performance.

1.2 This Work

The work presented in this thesis was inspired by the successful demonstration of high-power incoherent Raman pump sources, and the invention of the *New Design Method*. The basic idea is to study the performance of DCRA with incoherent pumps and the way of pursuing gain and OSNR flatness.

Another basic idea of this work is to investigate the system performance improvement by using incoherent pump source in comparison to the traditional coherent pump laser.

1.3 Thesis structure

The structure of the thesis is described in this section – for each chapter the main contents are described.

In *Chapter 2*, Basic definitions are given to describe a fiber Raman amplifier model. Corresponding to this physical model, a theoretical model is constructed by the basic equation that is used to calculate all the channel power while they propagate through the fiber. The propagation equation for each kind of channel (pump, signal, and ASE noise) is defined in forward and backward direction separately for greater

understanding, and verification is followed.

In *Chapter 3*, simulations based on the steady-state Raman model are done to a DCRA by using a conventional coherent pump. The example is taken from [16], and all the parameters used in this and the following simulations are conform to that. This is also for the purpose of making a better comparison. Then best DCF length is elucidated.

In *Chapter 4*, an incoherent pump source is applied to DCRA to pursue Gain flatness, with backward and forward pumping structures. In each pumping scheme, best results are obtained with one pump and two pumps, respectively.

In *Chapter 5*, an incoherent pump source is applied to DCRA to pursue OSNR flatness, with backward, forward pumping structures. In each pumping scheme, best results are obtained with one pump and two pumps, respectively.

Chapter 6 illustrates the trade-off relation between the gain and OSNR flatness by analyzing the results from the former chapters. Further bidirectional pumping regime is applied to achieve the best gain and OSNR flatness simultaneously.

Chapter 7 concludes this thesis and sums up all the results shown in previous chapters.

Chapter 2

Fiber Raman Amplifier Model

The property of Raman gain based on the frequency separation between pump and signal makes fiber Raman amplification widespread in the telecommunication spectrum. Therefore, fiber Raman amplifiers have been considered a flexible and simple way to amplify signal in both C and L band. Accordingly, the accuracy of fiber Raman amplifier modeling becomes extremely important, and many scientists have made their contributions in establishing and improving it. Stolen et al. [43] described modeling of Stokes amplified spontaneous emission (ASE) and multiple Stokes shifts in single-mode fiber. Kidorf et al. [44] gave detailed equations for a Raman amplifier model applied to single-mode optical fiber. Achtenhagen et al. [45] verified the gain predicted by this model, added Rayleigh backscattering and wavelength scaling approximation to account for effective fiber core area. Perlin et al. [5] added anti-Stokes spontaneous emissions. Berntson et al. [46] corrected the equation given by Kidorf in [44] for spontaneous absorption of signal photons. In this thesis, we use the Raman amplifier model for single-model optical fiber given in [38], which is the first explicit Raman propagation equations which include effects due to group velocity, MPI, as well as Stokes and anti-Stokes spontaneous emission.

In this chapter, basic definitions are given to describe a Raman amplifier model. Fundamental equation, which is used to calculate the powers of all channels

during their propagation, is explained explicitly. Propagation equations for all kinds of channels (pump, signal, and ASE noise) are listed before comparing our modeling with [38].

2.1 Basic definitions

Figure 2.1 illustrates a general fiber Raman amplifier. Parameters used to characterize the optical fiber are: length L; frequency dependent fiber attenuation $\alpha(\nu)$; Raman gain coefficient $g_R(\Delta\nu, \lambda_p)$, which depends on the frequency separation between beams, and the shorter wavelength between two channels; frequency dependent Rayleigh scattering coefficient $\gamma(\nu)$ and effective area of the fiber $A_{eff}(\nu)$; and absolute temperature T of the optical fiber. For the position reference, z is used, which is set to zero at the input end, and L at the output end. Signal and pump beams having photon numbers of n_i traveling in the forward and backward direction are written as n_i^+, n_i^-, respectively. Therefore, $n_i(0+)$ is the input, and $n_i(L+)$ is the output. If the pump beam is injected backwardly, it is denoted as $n_i(L-)$. Otherwise, it is included in the input side.

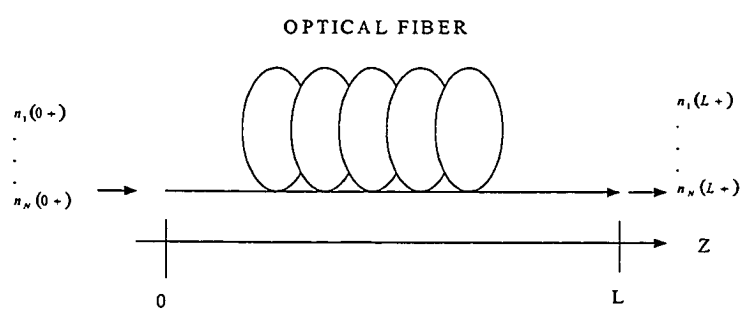

Figure 2.1 General Raman amplifier. $n_1(0+)..n_N(0+)$ are the number of photons in the forward traveling signal and pump beams at the input. Correspondingly, $n_1(0-)..n_N(0-)$ are the numbers of photons in the backward traveling ones at the output. L is the length of the optical fiber and z is the position in the fiber.

We use P_i to express the beam power for channel i in a limited bandwidth.

This channel i can be signal or pump, and P_i is defined in Equation (2.1), where ν_i is the frequency of the i-th channel. ASE noise power is calculated in a bandwidth of $\Delta\nu$. To indicate the difference, ASE noise power is denoted by P_i^{ASE}, and the definition is in Equation (2.2). Equation (2.3) is the relationship between Raman gain and Raman gain coefficient g_R.

$$P_i = h\nu_i n_i \tag{2.1}$$

$$P_i^{ASE} = \int_{\Delta\nu_i} n(\nu) h\nu d\nu \tag{2.2}$$

$$G(\nu_{signal}, \nu_{pump}) = g_R(\nu_{signal}, \nu_{pump}) \times P_{pump} \tag{2.3}$$

Raman gain is to indicate the amplification degree. The absolute gain from position z_1 to z_2 is defined in Equation (2.4), as P_s is the signal power at the two positions.

$$G_{absolute}(z_1 \to z_2) = \frac{P_s(z_2)}{P_s(z_1)} \tag{2.4}$$

The on-off Raman gain from position z_1 to z_2 is defined in Equation (2.5), which is the absolute gain minus fiber loss. Here α is in dB/km, and $L = z_1 - z_2$ is in km.

$$G_{on-off}(z_1 \to z_2)[dB] = G_{absolute}(z_1 \to z_2)[dB] - \alpha L \tag{2.5}$$

The noise figure of a Raman amplifier describes the noise performance, and it is defined by Equation (2.6) [47]. If the G is the on-off gain, the resulting noise figure is called equivalent noise figure (ENF).

$$F = \frac{1}{G}\left[\frac{P^{ASE+}(L)}{h\nu\Delta\nu} + 1\right] \tag{2.6}$$

Where $P^{ASE+}(L)$ is the forward ASE noise power in bandwidth of $\Delta\nu$ at the output end. Optical signal-to-noise ratio (OSNR) is defined as the ratio of the optical signal power to the power of ASE in a given reference bandwidth around the signal

wavelength.

$$OSNR = \frac{P_S(L)}{P^{ASE}(L)} \tag{2.7}$$

Where $P^{ASE}(L)$ is the ASE noise power at the output end in bandwidth of $\Delta\lambda$ (the resolution here is 1 nm) at the output end. $P_S(L)$ is the output signal power.

2.2 General model

Spontaneous Raman scattering was first discovered by Raman, who received the Nobel Prize in Physics in 1930 for this great contribution [36]. The physical process of spontaneous Raman scattering is as follows: an optical beam incident on a molecule makes the bound electrons of this molecule oscillate at the frequency of the optical beam. Hence, the oscillating dipole moment produces optical radiation at the same frequency with a phase shift. At the same time, the molecular structure itself is oscillating at the frequencies of various molecular vibrations. Therefore, the induced oscillating dipole moment contains the sum and difference frequency terms between the optical and vibrational frequencies. These terms give rise to Raman scattered light in the re-radiated field. Spontaneous Raman scattering is an isotropic process and occurs in forward and backward directions.

There are three types of Raman scattering processes:

- Pump photons give up their energy to create other photons of reduced energy at a lower frequency. The remaining energy is absorbed by silica molecules, which end up in an excited vibrational state. This is Stokes scattering. The vibrational energy levels of silica dictate the frequency shift ($\Omega_r = \omega_p - \omega_s$).

- Pump photon is absorbed by an excited molecule to emit a photon with energy equal to the sum of energies ($\Omega_r + \omega_p = \omega_{higher-frequency}$). This is called anti-Stokes scattering. It only takes place with a fiber temperature above the absolute zero.
- Signal photons absorbed by a molecule, which is in an excited state, will generate a pump photon ($\Omega_r + \omega_s = \omega_p$). This is inverse Stokes scattering.

Figure 2.2 describes the Raman scattering processes [41].

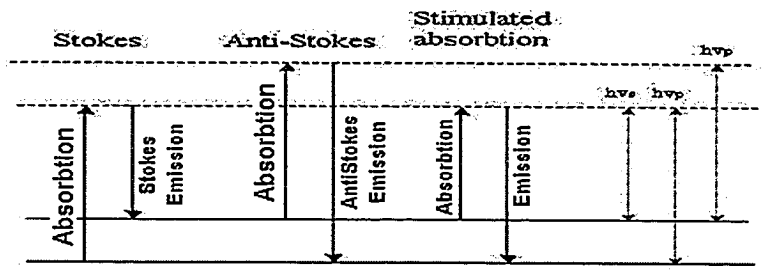

Figure 2.2: Energy diagram for the Raman scattering processes: Stokes scattering, anti-Stokes scattering and stimulated absorption. The energy differences between the levels are shown with dashed vertical lines on the right of the figure. The dashed horizontal lines show virtual levels. [41]

Stokes and anti-Stokes processes can generate new signal waves. These new waves can also work as pumps and create other new waves through Stokes or anti-Stokes. This is called higher-order Raman scattering, and will go on for an indefinite number of times. However, each Stokes or anti-Stokes conversion costs power, especially for anti-Stokes. Consequently, high order Stokes is not significant.

Stokes scattering can be used to amplify the signals if the frequency difference between signal and pump are within the Raman Stokes line region. This is the basic principle of a fiber Raman Amplifier. Moreover, Stolen found that Raman gain spectrum is temperature independent and anti-Stokes process occurs for an amplifier with fiber temperature greater than 0 K [37]. In today's commercially used silica fiber,

energy level covers a continuum broad bandwidth, not discrete frequency separation points [38]. The energy converting efficiency is expressed by Raman-gain coefficient (denoted by g_R, normalized gain coefficient $g_R = Raman\ gain\ cross\text{-}section / A_{eff}$). Raman-gain coefficients is an efficiency factor related to the gain, which determines the strength of the coupling between a pump beam and a signal beam due to stimulated Raman scattering. The scaling method of Raman gain coefficient (g_R) in this thesis is taken from [20].

In fact, inverse Stokes scattering is also an anti-Stokes process, which is different from anti-Stokes scattering only by the wavelength of absorbed photon. Pump photon is absorbed during anti-Stokes scattering process, while signal photon is absorbed during inverse Stokes scattering process. However, when considering the Raman interaction between two arbitrary bands, each of which is within a narrow bandwidth Δv and has single-mode polarized light, only two processes are included: Stokes scattering and anti-Stokes scattering. Between these two, Stokes scattering is responsible for Raman gain as well as pump depletion. Equation (2.7) is our base of Raman amplifier model given in [18] by Stokes and anti-Stokes analysis.

$$
\begin{aligned}
\pm \frac{dP_i^{\pm}}{dz} = & -\alpha(v_i, T)P_i^{\pm} && ① \\
& + \gamma(v_i)P_i^{\mp} && ② \\
& + P_i^{\pm}\sum_j^{v_j > v_i} g_R(v_j, v_i)[P_j^{+} + P_j^{-}] && ③ \\
& + 2\sum_j^{v_j \geq v_i}[P_j^{+} + P_j^{-}]h v_i \Delta v g_R(v_j, v_i) \times \left(1 + \frac{1}{e^{\frac{h(v_j - v_i)}{kT}} - 1}\right) && ④ \qquad (2.7) \\
& - P_i^{\pm}\sum_j^{v_j < v_i} \frac{V_j}{V_i}\frac{v_j}{v_i} g_R(v_i, v_j)[P_j^{+} + P_j^{-}] && ⑤ \\
& + 2\sum_j^{v_j < v_i}[P_j^{+} + P_j^{-}]h v_i \Delta v \frac{v_j}{v_i}\frac{V_j}{V_i} \times g_R(v_i, v_j)\frac{1}{e^{\frac{h(v_i - v_j)}{kT}} - 1} && ⑥
\end{aligned}
$$

Where h is Planck's constant, k is the Boltzmann constant, T is the temperature, v_j and v_i are the frequencies, V_i or V_j is group velocity denoted by subscript for different frequencies, and P_i^+ and P_i^- are the power at the i-th frequency in forward and backward, respectively. In the equation, ① and ② the present fiber loss and Rayleigh scattering; ③ is the gain from higher frequencies while ⑤is the depletion to lower frequencies; ④ and ⑥ are noises due to stimulated spontaneous emission, and anti-Stokes, respectively.

To apply this differential format equation to a fiber Raman amplifier with length L, the fiber can be separated into m segments, each of that has a length of $\Delta z = \frac{L}{m}$. Figure 2.3 gives the illustration.

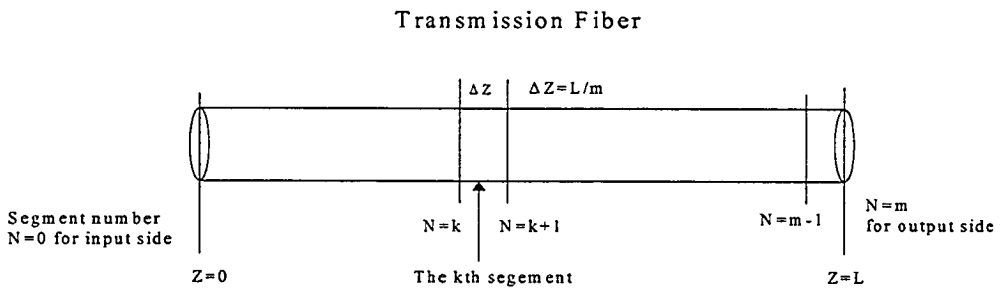

Figure 2.3 Transmission-fiber is separated into m segments to apply the integration in propagation equation.

Then, Equation (2.7) can be written as following in Equation (2.8).

$$\frac{dP_i^+(z_{k+1})}{dz} = -\alpha(\nu_i)P_i^+(z_k) + \gamma(\nu_i)P_i^-(z_k)$$
$$+ P_i^+(z_k)\sum_j^{\nu_j>\nu_i} g_R(\nu_j,\nu_i)\left[P_j^+(z_k) + P_j^-(z_k)\right]$$
$$+ 2\sum_j^{\nu_j>\nu_i}\left[P_j^+(z_k) + P_j^-(z_k)\right]h\nu_i\Delta\nu g_R(\nu_j,\nu_i)\times\left(1 + \frac{1}{\exp\left(\frac{h(\nu_j-\nu_i)}{kT}\right)-1}\right)$$
$$- P_i^+(z_k)\sum_j^{\nu_j<\nu_i}\frac{V_j}{V_i}\frac{\nu_j}{\nu_i}g_R(\nu_i,\nu_j)\left[P_j^+(z_k) + P_j^-(z_k)\right] \quad (2.8a)$$
$$+ 2\sum_j^{\nu_j<\nu_i}\left[P_j^+(z_k) + P_j^-(z_k)\right]h\nu_i\Delta\nu\frac{\nu_j}{\nu_i}\frac{V_j}{V_i}\times g_R(\nu_i,\nu_j)\left(\frac{1}{\exp\left(\frac{h(\nu_i-\nu_j)}{kT}\right)-1}\right)$$

$$\frac{dP_i^-(z_k)}{dz} = -\alpha(\nu_i)P_i^-(z_{k+1}) + \gamma(\nu_i)P_i^-(z_{k+1})$$
$$+ P_i^-(z_{k+1})\sum_j^{\nu_j>\nu_i} g_R(\nu_j,\nu_i)\left[P_j^+(z_{k+1}) + P_j^-(z_{k+1})\right]$$
$$+ 2\sum_j^{\nu_j>\nu_i}\left[P_j^+(z_{k+1}) + P_j^-(z_{k+1})\right]h\nu_i\Delta\nu g_R(\nu_j,\nu_i)\times\left(1 + \frac{1}{\exp\left(\frac{h(\nu_j-\nu_i)}{kT}\right)-1}\right)$$
$$- P_i^-(z_{k+1})\sum_j^{\nu_j<\nu_i}\frac{V_j}{V_i}\frac{\nu_j}{\nu_i}g_R(\nu_i,\nu_j)\left[P_j^+(z_{k+1}) + P_j^-(z_{k+1})\right] \quad (2.8b)$$
$$+ 2\sum_j^{\nu_j<\nu_i}\left[P_j^+(z_{k+1}) + P_j^-(z_{k+1})\right]h\nu_i\Delta\nu\frac{\nu_j}{\nu_i}\frac{V_j}{V_i}\times g_R(\nu_i,\nu_j)\left(\frac{1}{\exp\left(\frac{h(\nu_i-\nu_j)}{kT}\right)-1}\right)$$

Here, z_k is the k-th segment ($0 \le k \le m$). So, $P_i^+(z_0)$ is input signal and forward pump power (2.8a), and $P_i^+(z_m)$ is the output. If the Raman amplifier is backward pumped (2.8b), using $P_i^-(z_m)$ to indicate the inputted pump power.

2.3 Equations for signals, pumps, and ASE noise

For Raman amplifiers, inputs are signals and pumps. ASE noise is generated during the propagation. Figure 2.4 illustrates the wavelength distributions of signals,

pumps and ASE noise.

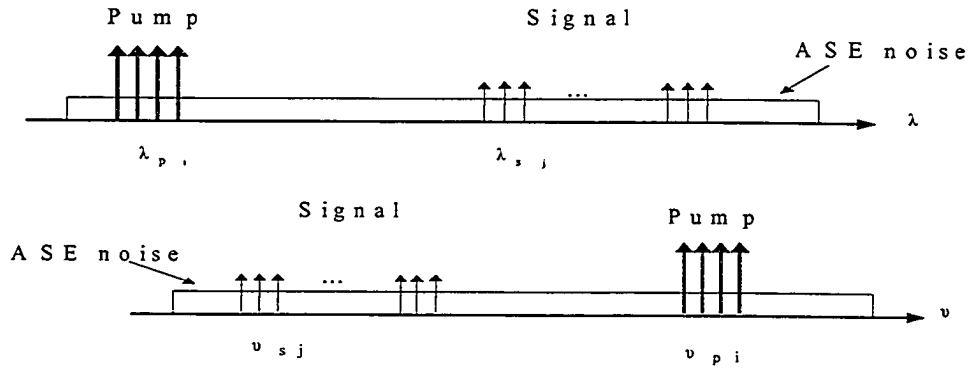

Figure 2.4 Wavelength distributions of signals, pumps, and ASE noises.

Signals obtain gains from pumps during the propagation. While they deplete their power by transferring energy to all of the longer wavelength channels (signals and ASE noise). SRS crosstalk between signals can be considered as gain or noise depending on cases. In this thesis, they are considered as gain because for CW wave inputs, and also SRS between signals are commonly taken as gain. When the DFRA has more than one pump, the pumps located at shorter wavelengths deplete their power to pump at all the longer wavelengths channels. Along with the propagation, signals can obtain power from generated ASE noise; however, the power is noise, and not gain; and also, the product from anti-Stokes process is noise. Based on the above considerations, we list signal, pump, and ASE noise propagation equations in Equation (2.9), Equation (2.10), Equation (2.11), respectively.

Signal equations: forward

$$\frac{dP_i^{+}(z_{k+1})}{dz} = -\alpha(\nu_i)P_i^{+}(z_k) + P_i^{+}(z_k)\sum_{j}^{\nu_j(pumps+signals)>\nu_i} g_R(\nu_j,\nu_i)\left[P_j^{+}(z_k)+P_j^{-}(z_k)\right] - P_i^{+}(z_k)\sum_{j}^{\nu_j(signals+noise)<\nu_i} \frac{V_j}{V_i}\frac{\nu_j}{\nu_i} g_R(\nu_i,\nu_j)\left[P_j^{+}(z_k)+P_j^{-}(z_k)\right] \quad (2.9)$$

Pump equations: forward

$$\frac{dP_i^{+}(z_{k+1})}{dz} = -\alpha(\nu_i)P_i^{+}(z_k) + \gamma(\nu_i)P_i^{-}(z_k)$$

$$+ P_i^{+}(z_k)\sum_{j}^{\nu_j(pumps)>\nu_i} g_R(\nu_j,\nu_i)\left[P_j^{+}(z_k)+P_j^{-}(z_k)\right]$$

$$- P_i^{+}(z_k)\sum_{j}^{\nu_j(pumps+signals+noise)<\nu_i} \frac{V_j}{V_i}\frac{\nu_j}{\nu_i} g_R(\nu_j,\nu_i)\left[P_j^{+}(z_k)+P_j^{-}(z_k)\right] \qquad (2.10a)$$

Pump equations: backward

$$\frac{dP_i^{-}(z_k)}{dz} = -\alpha(\nu_i)P_i^{-}(z_{k+1}) + \gamma(\nu_i)P_i^{+}(z_{k+1})$$

$$+ P_i^{-}(z_{k+1})\sum_{j}^{\nu_j(pumps)>\nu_i} g_R(\nu_j,\nu_i)\left[P_j^{+}(z_{k+1})+P_j^{-}(z_{k+1})\right]$$

$$- P_i^{-}(z_{k+1})\sum_{j}^{\nu_j(pumps+noise)<\nu_i} \frac{V_j}{V_i}\frac{\nu_j}{\nu_i} g_R(\nu_j,\nu_i)\left[P_j^{+}(z_{k+1})+P_j^{-}(z_{k+1})\right] \qquad (2.10b)$$

ASE noise power: forward

$$\frac{dP_i^{+}(z_{k+1})}{dz} = -\alpha(\nu_i)P_i^{+}(z_k) + \gamma(\nu_i)P_i^{-}(z_k)$$

$$+ P_i^{+}(z_k)\sum_{j}^{\nu_j>\nu_i} g_R(\nu_j,\nu_i)\left[P_j^{+}(z_k)+P_j^{-}(z_k)\right]$$

$$+ 2h\nu_i\Delta\nu\sum_{j}^{\nu_j>\nu_i} g_R(\nu_j,\nu_i)\left[P_j^{+}(z_k)+P_j^{-}(z_k)\right]\left[1+\frac{1}{\exp\left(\frac{h(\nu_j-\nu_i)}{kT}\right)-1}\right]$$

$$- P_i^{+}(z_k)\sum_{j}^{\nu_j<\nu_i}\frac{V_j}{V_i}\frac{\nu_j}{\nu_i} g_R(\nu_j,\nu_i)\left[P_j^{+}(z_k)+P_j^{-}(z_k)\right] \qquad (2.11a)$$

$$+ 2h\nu_i\Delta\nu\sum_{j}^{\nu_j<\nu_i}\frac{V_j}{V_i}\frac{\nu_j}{\nu_i} g_R(\nu_j,\nu_i)\left[P_j^{+}(z_k)+P_j^{-}(z_k)\right]\left[\frac{1}{\exp\left(\frac{h(\nu_i-\nu_j)}{kT}\right)-1}\right]$$

ASE noise power: backward

$$\frac{dP_i^-(z_k)}{dz} = -\alpha(\nu_i)P_i^-(z_{k+1}) + \gamma(\nu_i)P_i^+(z_{k+1})$$

$$+ P_i^-(z_{k+1})\sum_j^{\nu_j>\nu_i} g_R(\nu_j,\nu_i)[P_j^+(z_{k+1}) + P_j^-(z_{k+1})]$$

$$+ 2h\nu_i\Delta\nu\sum_j^{\nu_j>\nu_i} g_R(\nu_j,\nu_i)[P_j^+(z_{k+1}) + P_j^-(z_{k+1})]\left[1 + \frac{1}{\exp\left(\frac{h(\nu_j-\nu_i)}{kT}\right)-1}\right]$$

$$- P_i^-(z_{k+1})\sum_j^{\nu_j<\nu_i}\frac{V_j}{V_i}\frac{\nu_j}{\nu_i} g_R(\nu_j,\nu_i)[P_j^+(z_{k+1}) + P_j^-(z_{k+1})] \qquad (2.11b)$$

$$+ 2h\nu_i\Delta\nu\sum_j^{\nu_j<\nu_i}\frac{V_j}{V_i}\frac{\nu_j}{\nu_i} g_R(\nu_j,\nu_i)[P_j^+(z_{k+1}) + P_j^-(z_{k+1})]\left[\frac{1}{\exp\left(\frac{h(\nu_i-\nu_j)}{kT}\right)-1}\right]$$

To verify the correctness of our modeling, we repeat the same simulations as given in [18]. Verification 1 is based on a 13-km TW-Reach transmission fiber at 300 K temperature. Input is a 13mW signal at wavelength of 1560 nm. Figure 2.5 is the comparison of the results between [18] and our modeling. Since Figure 2.5 (a) is based on TW-RS fiber, while Figure 2.5 (b) is based on TW-Reach fiber, and it is clear that Figure 2.5 (a) and (b) have the same power density shape but with different absolute values due to different fibers.

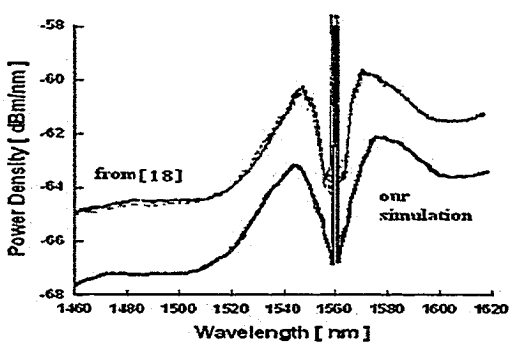

Figure 2.5 Power spectrum comparisons from [18] and our work.

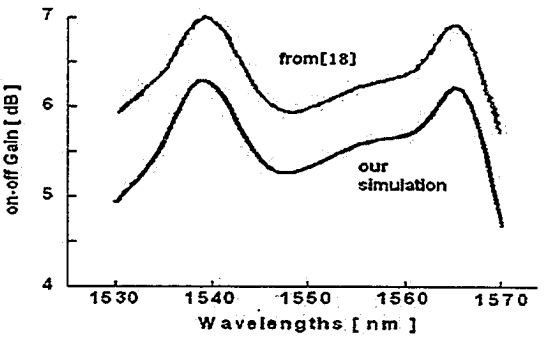

Figure 2.6 On-off gain comparisons from [18] and our work. SRS between signals is noise, and MPI is not considered.

Verification 2 is to use a 100 km Corning SMF-28 fiber, with input of 51 channels in C band, each of which has a power of 1.96 mW. The channel spacing is 100 GHz. Two pumps are co-injected with 300 mW at 1430 nm and 262.5 mW at 1454 nm. Moreover, SRS between signals is considered as noise and MPI is not considered according to [18]. Figure 2.6 shows the comparison of on-off gain between [18] and our work. Gain spectrums in Figure 2.6 (a) and (b) are completely the same except that the gain in (b) is about 1 dB smaller than the gain in (a). The difference in absolute gain values may be due to the different g_R values (we do not have the same g_R as in [18]). Therefore, we confirmed the correctness of our modeling. The assumptions of this thesis are: SRS between signals is considered as gain, and MPI is considered noise. We repeat the simulation of verification 2 with taking SRS between signals as gain and MPI as noise, and the gain spectrum is illustrated in Figure 2.7. From the spectrum in Figure 2.7, we see that SRS between signals has a significant impact on gain spectrum.

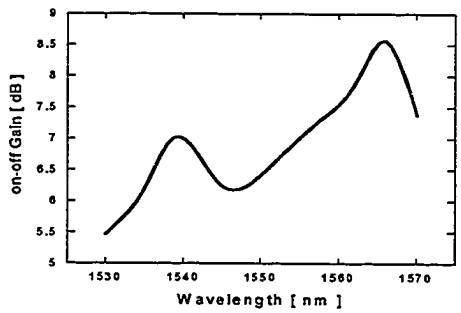

Figure 2.7 Gain spectrum from our work, SRS between signals is gain, and MPI is considered.

Chapter 3

Gain flatness of FRA's with coherent pumps

In the broadband Raman Amplifiers, the noise performance of the shorter wavelength signal is found to be significantly worse than the longer wavelength signal for purely backward pumping scheme which was commonly used nowadays. The reason is due to several factors: pump-pump Raman interaction, signal-signal Raman interaction, and proximity of signal to the pump and wavelength dependent fiber loss. By using a piece of DCF Fiber as the discrete amplifier, the noise performance is improved [49] ~ [52].

The DCF based discrete Raman amplifier is used to provide additional gain to compensate the loss from DCF and other passive/active optical components. In this chapter, simulations of dispersion compensating Raman amplification using conventional coherent pumps are performed. The results are given for comparison with the following chapters.

3.1 Gain flatness of FRA's with coherent pumps

The *New Design Method* proposed in [16] improved the system noise performance by moving part of the gain at long wavelength side of the distributed fiber to the short wavelength side of the following discrete amplifier. To give a

general and exact example of gain and OSNR flatness using coherent pump and further verify the correctness of our modeling, we repeat the same simulations as given in [16]. Here we use 80 km of TW-Reach fiber as the transmission fiber and 8 km of DCF as the gain medium of a discrete Raman amplifier. Both the transmission fiber and the DCF are backward pumped by six coherent Raman pumps. The parameters on the six pumps are listed in Table 3.1. We use 122 signals (from 1515 to 1615 nm with 100 GHz channel spacing) with input power of -2 dBm (0.63 mW) per channel in our simulation. The simulation results from [16] and our work are shown in Figure 3.1 and 3.2. Figure 3.1 gives the distributed Raman gain. The gain here we are using refers to on-off gain, and noise figure refers to equivalent noise figure from this chapter on, for convenience. Detail definition refers to *Chapter 2*. And the total gain output of the two-stage DCRA is defined as follows: $G_{Total} = 10 \log\left[\frac{P_{output}}{P_{input}}\right] + Loss_{Trs}$, where $Loss_{Trs}$ stands for the loss from the transmission fiber. Total noise figure is defined as: $NF_{Total} = NF_1 + \frac{1}{G_1}[NF_2 - 1]$, where NF_1 stands for the noise figure from the first stage, NF_2 stands for the noise figure from the second stage, and G_1 stands for the gain from the distributed Raman amplifier. System 1 is the common design, where the gain profiles in both the distributed and discrete Raman amplifiers are flattened. System 2, 3, 4 are new designs with different gain distributions. The total gain of the system output is about the same with the gain from the System 1. Figure 3.2 shows the corresponding OSNR of the four systems. We see that with using the *New Design Method*, the ripple of

OSNR is lessened from 8 dB (System 1) to less than 2 dB (System 4).

λ (nm) / P (mW)		1412	1425	1436	1452	1466	1496	Total Power
I	TW-Reach	397	188	169	57	47.8	27	1294.8
	DCF	137	67	71	35	43	56	
II	TW-Reach	338	154	121	43.6	38	13	1224.9
	DCF	96.7	56	100	44	42.6	178	
III	TW-Reach	313	140	103	39	34	7.6	1207.6
	DCF	57	44	121	50	43	256	
IV	TW-Reach	288	127	88.5	34.6	32	2.6	1197.7
	DCF	2	26	146	58	44	349	

Table 3.1: Parameters used in the simulation with coherent pumps

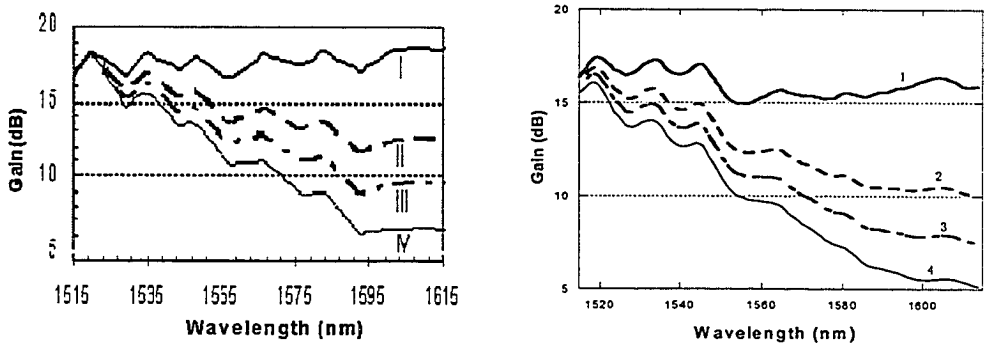

(a) (b)

Figure 3.1 Raman gain from the distributed Raman amplifier: (a) from [16]; (b) our work

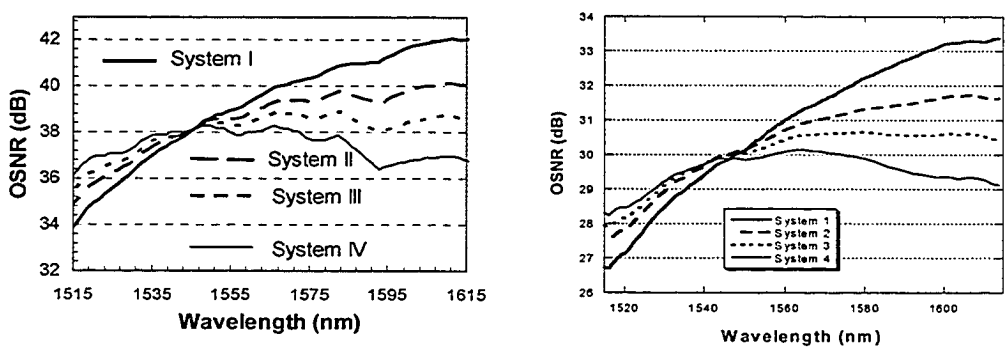

(a) (b)

Figure 3.2 Corresponding OSNR from the distributed Raman amplifier: (a) from [16]; (b) our work

From the Figure 3.1 and Figure 3.2, we see that the results from our work match [16] for the overall trends, but with a slight difference of the individual value. This is because the scaling methods of the Raman gain coefficient that we used are different from [16]. We use the latest scaling method given in [20]. What's more, the spacing of the ASE spectrum used in the simulation is not the same.

So far, we can draw two conclusions from the results above:

1. To achieve gain flatness on the dispersion compensated Raman module within 100 nm bandwidth, six pumps are needed to obtain a gain ripple of 2 dB.
2. The OSNR flatness can be gained from the *New Design Method* by pushing up the value at the shortest wavelengths and pulling it down at the longest wavelengths.

3.2 Best DCF Length

Dispersion compensating fiber (DCF) was originally used as a way of compensating chromatic dispersion along the transmission produced by the natural characteristic of the optical fiber. But later it was found out that it could be a good Raman gain medium because DCF has a high Germanium concentration and a small mode field area; this increases the Raman gain efficiency and saves pump power. It is also attractive to incorporate the dispersion compensation along with loss compensation in a transmission fiber span, or in other words to produce a dispersion compensation module to provide extra gain for long-haul and ultra-long-haul WDM

transmission span.

However, there is a bargain on the best DCF length used in the system. As a Raman amplifier, DCF can not be so short, because Raman scattering is a fast process, there are no long upper-state lifetimes to buffer pump fluctuations. For the reason of efficiency, Raman amplifiers typically consist of several kilometers of fiber. Then, a given portion of signal light can pass through many pump fluctuations if the signal and pump propagate in opposite directions, or if they forward propagate at different velocities. This averaging effect can reduce the impact of pump fluctuations [3]. And DCF can not be so long, either, as more MPI and other nonlinearities will be produced. In order to decrease the nonlinearity from the discrete Raman fiber amplifier, and to prevent MPI degradation, the DCF length needs to be kept at less than 10 km.

We use 8 km of the DCF in our simulation in order to keep the consistency with the example, and also for a better comparison upon the following simulation results. It was found that for ~8 km of the DCF, the net peak gain of up to ~ 7 dB (including coupling loss) is allowed keeping the optical signal to noise ratio more than 40 dB [49]. Actually, different DCF lengths were used in the related publications according to practical applications [49] ~ [52].

3.3 Summary

This chapter has investigated the gain and OSNR flatness in dispersion compensating fiber Raman amplification module using coherent pumps with a *New Design Method.* Simulations are done based on the examples in [16] and the results

are given. We see that the results from our work match the examples well, with a slight difference, and the reason is explained. The overall OSNR flatness is significantly improved, the ripple is reduced to less than 2 dB from the normal case of 8 dB. This increases the stability and system performance.

Then best DCF length is elucidated. We take 8 km as our DCF length in the simulations of this and following chapters to conform to the example and to make a better comparison all through the thesis.

The conclusions in this chapter are:

1. To have a gain ripple of less than 2 dB in the **coherent** pumped dispersion compensated Raman amplifier, at least **6 pumps** are necessary.
2. *New Design Method* can improve the OSNR flatness significantly.

The results will be used in the following chapters to compare to the case using incoherent pump source and to pursue both gain and OSNR flatness.

Chapter 4

Gain Flatness of FRA's with incoherent pumps

An incoherent pump is a new fabricated Raman amplifier pump source provided by the *Ahura*® Corporation in the year 2003. In this chapter, first the incoherent pump theory and its modeling method used in this thesis are explained. Then the applications using this pump source to pursue gain flatness with both forward and backward pumping scheme are demonstrated.

4.1 Incoherent pump theory and modeling

4.1.1 Introduction of incoherent pump

An incoherent pump beam is a pump that spreads its power within a broad bandwidth, not within a narrow bandwidth like a coherent pump beam. This broadband pump is achieved by coupling a low-power seed optical signal into a long-cavity semiconductor amplifier waveguide. This method is called the seeded power optical amplifier (SPOA) concept. A semiconductor optical amplifier is designed and fabricated to have saturated output power of > 250 mW currently [15], and could be further increased. Figure 4.1 is a photograph of high-power broad bandwidth Raman pump module [23]. Within the butterfly package, seeded source input, optical amplifier devices, isolators, detectors, and thin-film signal/pump WDM

optics are integrated. Figure 4.2 is an optical spectrum of an on-sale incoherent pump.

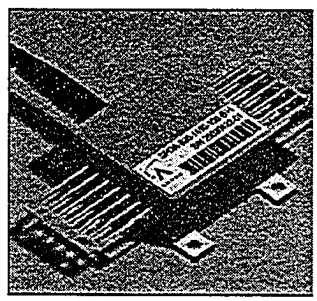

Figure 4.1 High-power broadband Raman pump module [23]

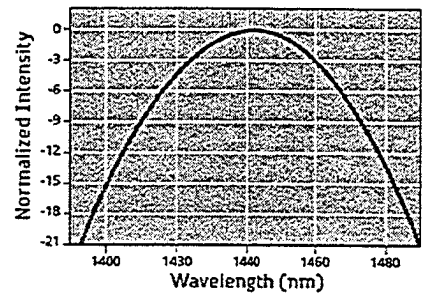

Figure 4.2 Optical-spectrum of an incoherent pump on sale [23].

From the introduction given by *Ahura*®, we know that by adjusting the central wavelength and input current of the pump model, the required incoherent pump can be obtained easily. At the moment, *Ahura*® Corporation provides incoherent pumps with central wavelength between 1440 nm and 1460 nm, FWHM bandwidth of greater than or equal to 35 nm, and minimum output power of 125 mW. The residual polarization was less than 1% and the Relative Intensity Noise (RINs) was less than -140 dB/Hz.

In the thesis, incoherent pumps are not restricted to the current commercial products. We simply investigate dispersion compensated Raman amplification modules with incoherent pumps that provide good performance.

4.1.2 Modeling of incoherent pump

An incoherent pump is modeled as follows. The Gaussian noise is generated in a broad bandwidth. After the noise passes through a Gaussian filter, we obtain a Gaussian-intensity spectrum. The incoherent pump is adjustable by changing the center wavelength, FWHM bandwidth of the filter and the power of Gaussian noise.

Equation (4.1) is the Gaussian filter equation.

$$H(\lambda) = Exp\left[-\frac{1}{2}\frac{(\lambda-\lambda_\gamma)^2}{\lambda_0^{\,2}}\right] \tag{4.1}$$

Where λ_0 is the central wavelength.

Figure 4.3 is an example of a simulated incoherent pump. The filter is centered at 1453 nm, with FWHM bandwidth equal to 35 nm. The Gaussian noise power is around 3.31 mW within 1 nm bandwidth. Letting the Gaussian noise pass through the above filter, we obtain the incoherent pump shown in Figure 4.3. Its total power is 230 mW and spreads from 1405 nm to 1498 nm. Figure 4.4 shows the on-off Raman gain after a 50 km TW-Reach fiber, which is backward pumped by the above incoherent pump and the coherent pump with the same power located at 1453 nm.

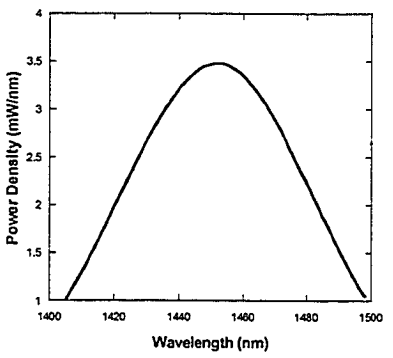

Figure 4.3 Incoherent pump example: central wavelength 1453 nm, FWHM bandwidth 35 nm, total power 230 mW.

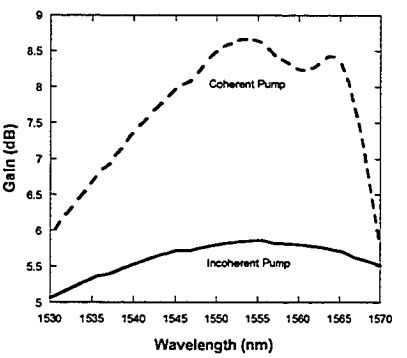

Figure 4.4 Gain comparison: The pump power is 230 mW. Incoherent pump is solid curve. Dash curve is coherent pump located at 1453 nm.

Figure 4.4 shows that an incoherent pump provides a more flat gain than a coherent pump with the same power. The example shows that gain ripple by an incoherent pump is 0.8 dB, while the smallest gain ripple is 2.7 dB from a coherent

pump with 230 mW. However, gain values resulting from an incoherent pump are much smaller than the values from a coherent pump. The reason for this phenomenon is that an incoherent pump spreads its power in a broadband range and amplifies signals in a broader wavelength range. Consequently, gain becomes smaller.

4.2 Gain flatness of FRA's with backward pumping scheme

The schematic of backward pumping is shown in Figure 4.5. In this configuration, an 80 km TW-Reach fiber was used as the transmission fiber and 8 km of DCF as the gain medium of a discrete Raman amplifier. The reason why DCF was kept shorter than 10 km is because longer DCF tends to cause more multi-path interference (MPI) and produces more non-linearity (see *Chapter 3*). Both the transmission fiber and DCF are backward pumped by an incoherent pump source with adjustable total pump power.

We use 122 signals in 100 nm bandwidth covering C-band and L-band (from 1515 to 1615 nm with 100 GHz channel spacing) with input power 0.63 mW(-2 dBm) per channel in our simulation.

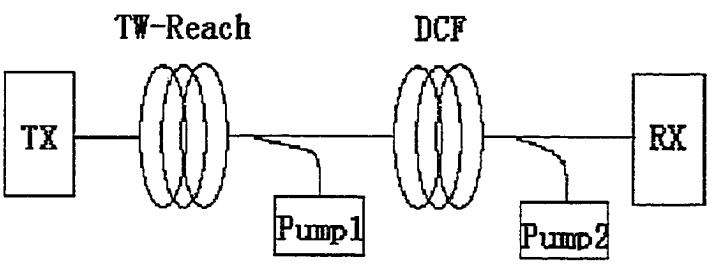

Figure 4.5 Schematic of backward pumping scheme

4.2.1 One pump

Basically, in the dual-stage Raman amplifier, namely a distributed amplifier followed by a discrete one, the total gain output is the superposition of the two--not the absolute value summation, but the trends multiply. In other words, any change from the separate gain will affect the total gain output. In order to demonstrate this, two incoherent pumps were chosen randomly, simulation was done with backward pumping scheme, and the results are shown in Figure 4.6. Figure 4.6(a) shows the contribution of each gain to the total gain output, and their relationships; Figure 4.6(b) gives the corresponding noise figure and OSNR level. This is also a general example of simulation using incoherent pumps in backward pumping dual-stage Raman module—dispersion compensation Raman amplifier.

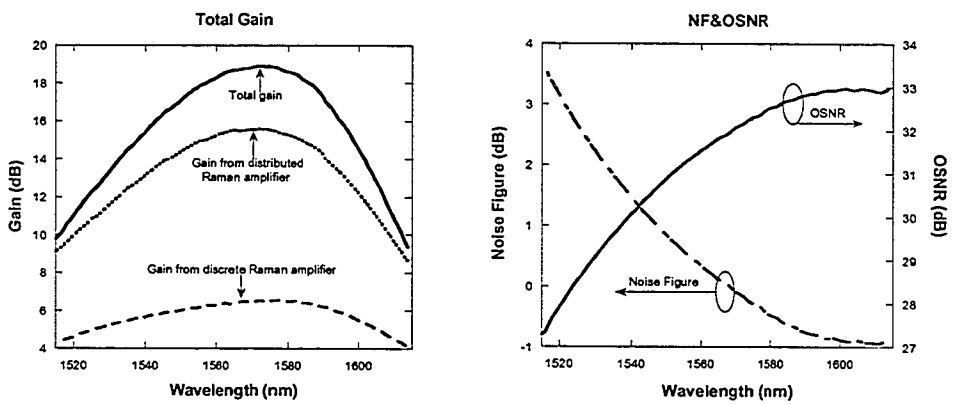

Figure 4.6 (a) Total gain output of a DCRA from a general example; (b) Corresponding noise figure and OSNR

Figure 4.7 (a) shows the gain flatness with one incoherent backward pump. The pump power used in the distributed Raman amplifier (TW-Reach fiber) is 454

mW, the center wavelength of this pump is 1420 nm, and the FWHM of this pump is 28 nm. For the discrete Raman amplifier (DCF fiber), the pump power is 295.5 mW, the center wavelength is 1497 nm, and the FWHM is 9 nm. Figure 4.7 (b) shows the corresponding average noise figure and OSNR level. The ripple of total gain is 2 dB, which can be obtained by using at least 6 pumps if a coherent pump source is to be used. With further adjustment and optimization to the parameters, better results could possibly be achieved. The ripple of the OSNR is about 2.5 dB, which is good for the average level of 29 dB. The noise figure is less than 2.1 dB.

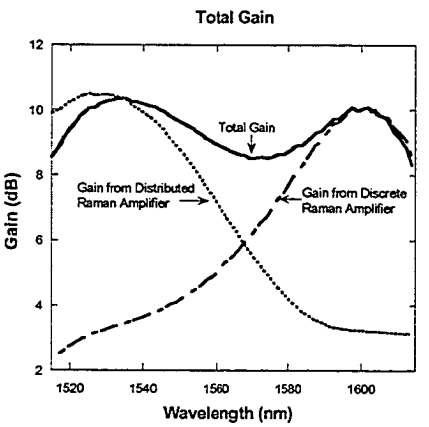

Figure 4.7 (a) Gain output from one pump backward pumping scheme;

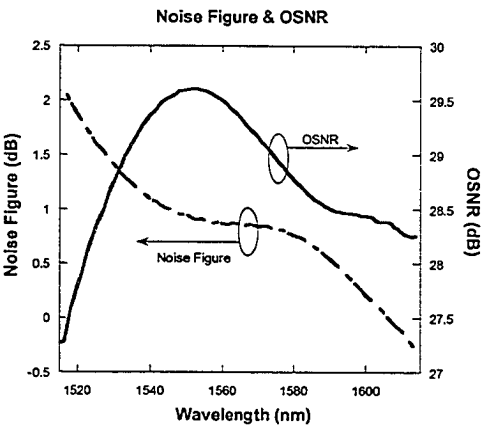

(b) Corresponding noise figure and OSNR

4.2.2 Two pumps

The schematic of two pumps backward pumping is the same as in Figure 4.5. The only difference is that both pump 1 and pump 2 are composed of two incoherent pumps.

Figure 4.8 (a) shows the gain flatness with two incoherent backward pumps, all the parameters used in this simulation are listed in Table 4.1. Figure 4.8 (b) gives the corresponding gain and noise figure value results in the simulation. The ripple of

gain is 0.8 dB, which is a much better result than that can be achieved with one pump. And this is very small for all the current applications in the transmission systems. Also, this is the smallest ripple for a two-stage Raman amplifier to our knowledge. The ripple of the OSNR is about 1.2 dB, which is very good for pure backward pumping.

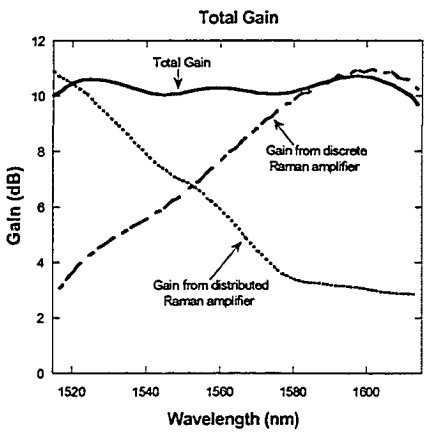

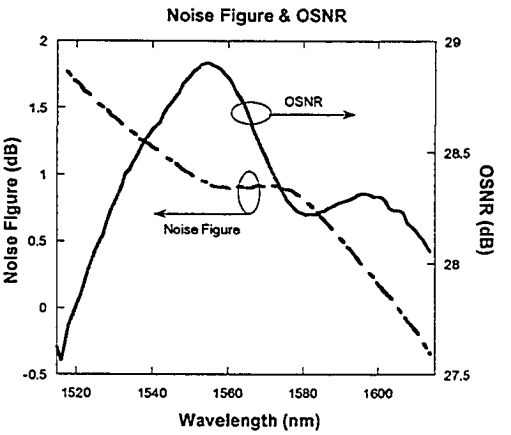

Figure 4.8 (a) Gain output from two pumps Backward pumping scheme; (b) Corresponding noise figure and OSNR

		Center Wavelength (nm)	FWHM (nm)	Total Pump Power (mW)
Pump for TW-Reach	Pump1	1400	28	536
	Pump2	1447	15	
Pump for DCF	Pump1	1478	17	402
	Pump2	1508	7	

Table 4.1 Parameters used in the backward pumping simulation with two incoherent pumps

The energy is transferred from a pump to a longer wavelength pump via Raman process in a multi-pump scheme, so the gain profile is asymmetric: the longer wavelength will have more gain. The traditional methods use narrower band gap and/or more power allocation to shorter wavelength to realize a flat, broadband Raman gain. Still, in the incoherent pump case, as we can see from table 4.1, the

power density of shorter wavelength is larger, while power density at longer wavelength is smaller.

4.3 Gain flatness of FRA's with forward pumping scheme

There is a source of noise that arises from the short upper-state lifetime of Raman amplification, as short as 3 to 6 fs. This virtually instantaneous gain can lead to a coupling of pump fluctuations to the signal. The usual way of avoiding this deleterious coupling is to make the pump and signal backward propagating, which has the effect of introducing an effective upper-state lifetime equal to the transit time through the fiber. If forward propagating pumps and the signals are to be used, the pump lasers must be very quiet. That is, they must have a very low so-called relative intensity noise (RIN). The development of low RIN, spectrally broadened incoherent pump makes it possible to have a new look at the forward pumping for Raman amplifiers. Basically, the principle of Raman pumping mechanism has nothing to do with direction. It just deals with the frequency offset between pumps and signals. But different pumping propagation has varied consequences. In backward pumping, because of the fiber attenuation, both pump and signal powers are somehow averaged along the transmission fiber. This potentially avoids the degradation from nonlinearities. Whilst for forward pumping, signal and pump powers are both high at the front end of the transmission fiber, and drop at the comparative rate along the fiber. At the front end, high power causes more RIN transfer. At the back end, low power leads to lower pumping efficiency. These are some reasons why backward pumping is

used more widely than forward pumping in the applications. Besides, there are other advantages which backward pumping has over forward pumping. But forward pumping also has some benefits. For example, it can improve the optimum Bit Error Rate (BER), because to achieve high forward gain, input signal power needs to be lower. This reduces distortions from signal nonlinearities. And what's more, when used in the discrete Raman amplifier, forward pumping can have a better noise performance at the front end than backward pumping.

Forward pumping is also beneficial in terms of MPI generated. A large amount of MPI is induced by double Rayleigh backscattering (DRB). Moving gain before loss (to the front of the span) ensures that any DRB light that is amplified by the full Raman gain at both ends must have also double-passed the net loss of the fiber in the center. If the gain arises after loss, only part of amplified DRB light is attenuated by fiber loss thus inducing more MPI. Therefore, less DRB light is produced for the same amount of gain if forward pumping is used [25]. In this thesis forward pumping regime was employed in the simulation to show another possibility of obtaining a better flattening approach.

The schematic of forward pumping is shown in Figure 4.9. All the parameters are as the same as described in section 4.2.

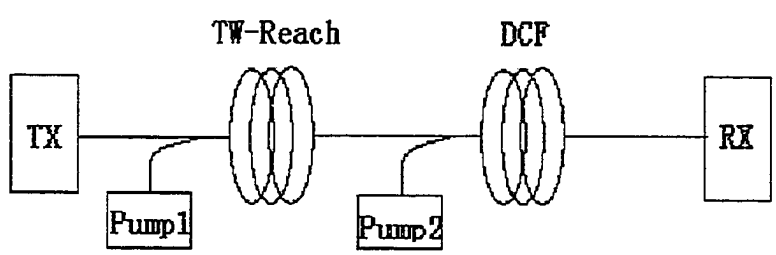

Figure 4.9 Schematic of forward pumping scheme

4.3.1 One pump

Figure 4.10 (a) shows the gain flatness with one incoherent forward pump. The pump power used in the distributed Raman amplifier (TW-Reach fiber) is 454 mW, the center wavelength of this pump is 1410 nm, and the FWHM of this pump is 35 nm. For the discrete Raman amplifier (DCF fiber), the pump power is 225.5 mW, the center wavelength is 1496 nm, and the FWHM is 10 nm. Figure 4.10 (b) shows the corresponding noise figure and OSNR level. The ripple of total gain is 2 dB. With further adjustment and optimization to the parameters, better results could be achieved. The ripple of the OSNR is about 3 dB. The noise figure is less than –3 dB through the whole 100 nm band width.

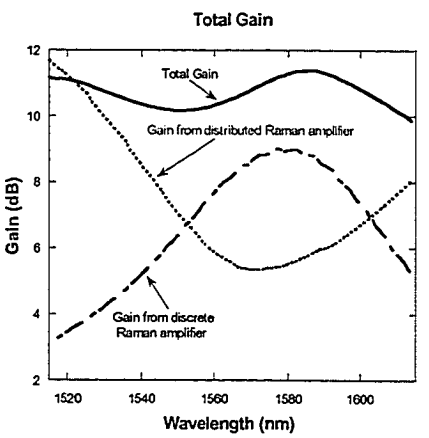

Figure 4.10 (a) Gain output from one pump forward pumping scheme;

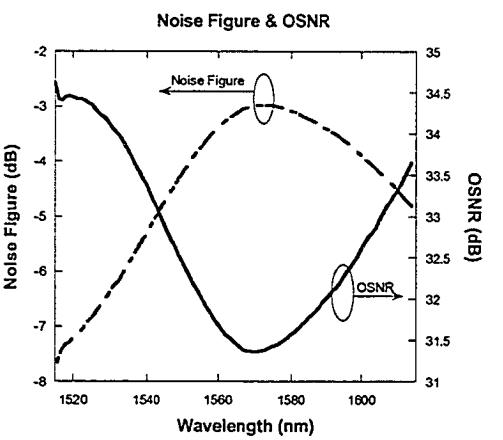

(b) Corresponding noise figure and OSNR

4.3.2 Two pumps

Figure 4.11 (a) shows the gain flatness with two incoherent forward pumps, all the parameters used in this simulation are listed in Table 4.2, and Figure 4.11 (b) gives

the corresponding noise figure and OSNR value result in the simulation. A total pump power of 717.5 mW was used for the transmission fiber, and up to 241 mW was launched into DCRA. For obtaining similar gain level, a little higher pump power is needed here than in the backward propagating case. The average gain level here is 10.5 dB and the gain ripple is less than 0.8 dB. With further optimization of pump wavelengths and configuration, it is possible to obtain a flatter gain spectrum, and better pump efficiency.

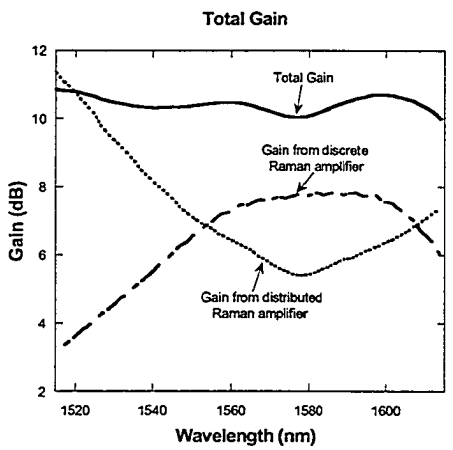

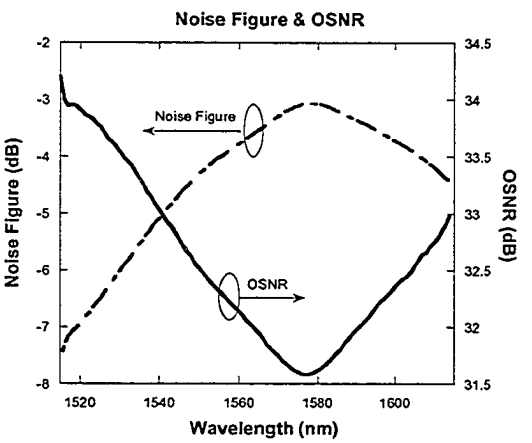

Figure 4.11 (a) Gain output from one pump; forward pumping scheme

(b) Corresponding noise figure and OSNR

		Center Wavelength (nm)	FWHM (nm)	Total Pump Power (mW)
Pump for TW-Reach	Pump1	1400	24	717.5
	Pump2	1450	10	
Pump for DCF	Pump1	1460	15	241
	Pump2	1495	12	

Table 4.2 Parameters used in the backward pumping simulation with two incoherent pumps

From the figures above, we can also see that backward pumping has a noise figure greater than 0 dB for over 90% of the bandwidth, whilst forward pumping brings it down to -3 dB or less all through the whole 100 nm band. This is because the

same propagation direction of pump and signal in forward pumping gives a higher pumping efficiency. In backward pumping, the pumping efficiency is higher when longer wavelength pumps receive more power transferred from shorter wavelengths. It clearly demonstrates that comparable noise performance improvement (hence the OSNR improvement) could be achieved with forward pumping, in comparison to backward pumping. We will see more of this in the next chapters.

4.4 Summary

This chapter has investigated the methods of obtaining gain flatness with forward and backward pumping scheme using a broadband incoherent pump source. The treatment has focused on dispersion compensated Raman amplification module for use in long-haul transmission systems, mainly of a typical terrestrial span length of 80 km.

The incoherent pump source and its modeling method were first introduced. Then a backward pumping scheme was used to pursue the gain flatness. We see that with one incoherent pump a gain ripple of 2 dB was obtained; and with two incoherent pumps, a gain ripple of 0.8 dB was achieved. Note that if a conventional coherent pump was used, as much as 6 pumps and 12 pumps would be needed for the ripple of 2 and 1 dB, respectively[16][24].

Lastly, a forward pumping regime was employed in the simulation. We see that with one incoherent pump a gain ripple of 2 dB was acquired; and with two incoherent pumps, a gain ripple of 0.8 dB was achieved.

We can conclude that by applying an incoherent pump source, a better gain flatness was achieved with fewer pumps. As far as the gain flatness is concerned, forward and backward pumping possess almost the same performance; comparable OSNR improvement could be achieved with forward pumping, in comparison to backward pumping. In the next chapter, we will investigate the OSNR flatness with an incoherent pump on the dispersion compensated Raman amplifier in detail.

Chapter 5

OSNR Flatness of FRA's with incoherent pumps

Raman Amplification has been proven to provide better OSNR, wider bandwidth and flatter gain profile than conventional amplifiers based on EDFA. The improved OSNR by Raman amplifier enables higher transmission capacity and longer reach. Optical signal-to-noise ratio (OSNR) is defined as the ratio of the optical signal power to the power of ASE in a given reference bandwidth (often 0.1 nm) around the signal wavelength. For the high capacity WDM transmission systems, flat OSNR performance within a wide wavelength band (such as 100 nm) over typical terrestrial span lengths of 80 to 100 km is the same or even more important than gain flatness, because transmission performance is mainly determined by OSNR, and all the efforts done before were eventually to pursue a relatively steady output. For the combined structure, namely distributed Raman amplifier followed by a discrete Raman amplifier (dispersion compensation fiber), the OSNR is analytically evaluated at the end of the system-the DCF output. In this chapter, simulations will be presented to obtain the OSNR flatness with both backward and forward pumping regime.

5.1 OSNR flatness of FRA's with backward pumping scheme

5.1.1 One pump

Figure 5.1 (a) shows the OSNR flatness with one incoherent backward pump. The pump power used in the distributed Raman amplifier (TW-Reach fiber) was 572.7 mW, the center wavelength of this pump was 1410 nm, and the FWHM of this pump was 28 nm. For the discrete Raman amplifier (DCF fiber), the pump power was 189.8 mW, the center wavelength was 1470 nm, and the FWHM was 28 nm. So the total pump power used here was 752.5 mW, and Figure 5.1 (b) shows that the average gain level is around 10 dB. The ripple of OSNR is less than 1.5 dB, which is a very good result that can be achieved with one pump. The ripple of the total gain is about 9 dB, which is not acceptable. The noise figure is less than 1.5 dB through the whole 100 nm band.

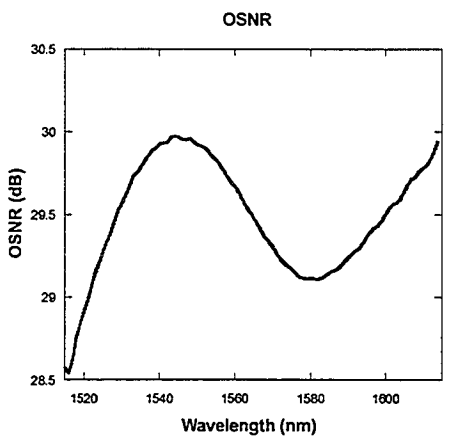

Figure 5.1 (a) OSNR flatness result using one pump in the backward pumping scheme;

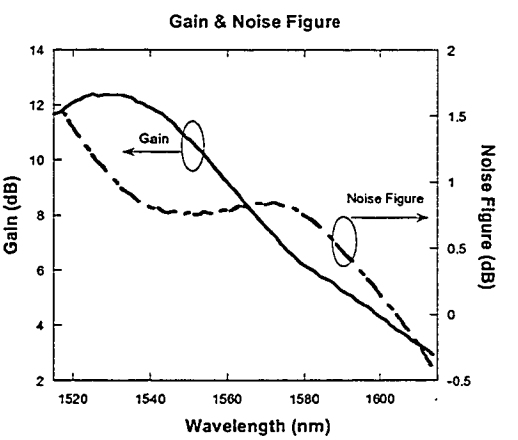

(b) Corresponding gain and noise figure

5.1.2 Two pumps

Figure 5.2 (a) shows the OSNR flatness with two incoherent backward pumps, all the parameters used in this simulation are listed in Table 5.1, and Figure 5.2 (b) gives the corresponding gain and noise figure value result in the simulation. The ripple of OSNR is 0.8 dB, which is a much better result than what can be achieved with one pump. And this is very small for the average OSNR level of about 30 dB. The ripple of the total gain is about 9 dB, which is not acceptable in real applications.

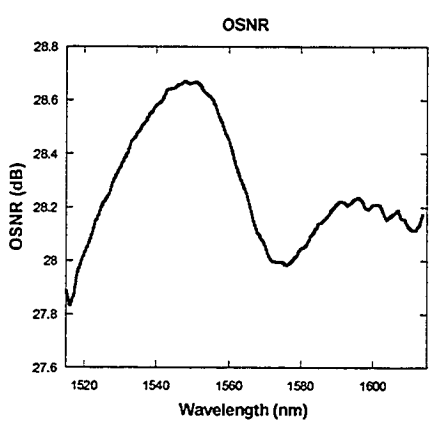

Figure 5.2 (a) OSNR flatness result using two pumps in the backward pumping scheme;

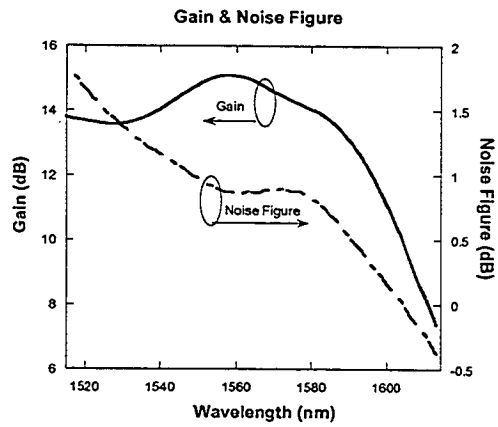

(b) Corresponding gain and noise figure

		Center Wavelength (nm)	FWHM (nm)	Total Pump Power (mW)
Pump for TW-Reach	Pump1	1400	28	536
	Pump2	1447	15	
Pump for DCF	Pump1	1460	15	602
	Pump2	1489	12	

Table 5.1 Parameters used in the backward pumping simulation with two incoherent pumps

Note that for backward pumping scheme, the OSNR value takes its lowest value at the shortest wavelength, and goes up gradually; this is spontaneously unavoidable for purely backward pumping regime, because at a low frequency window, the signal power experiences more gain, whilst when the frequency moves to

a higher window, more and more power transfers to ASE which causes degradation of OSNR at the low wavelength window.

5.2 OSNR flatness of FRA's with forward pumping scheme

5.2.1 One pump

Figure 5.3 (a) shows the OSNR flatness with one incoherent forward pump. The pump power used in the distributed Raman amplifier (TW-Reach fiber) is 612 mW, the center wavelength of this pump is 1400 nm, and the FWHM of this pump is 30 nm. For the discrete Raman amplifier (DCF fiber), the pump power is 635 mW, the center wavelength is 1501 nm, and the FWHM is 8 nm. Figure 5.3 (b) shows the corresponding average gain and noise figure level. The ripple of OSNR is less than 2 dB—a little higher than the former case using one backward pump, but they are all in a normal scope. With further adjustment and optimization to the parameters, better results could be achieved. The ripple of the total gain is about 9 dB, which is not acceptable.

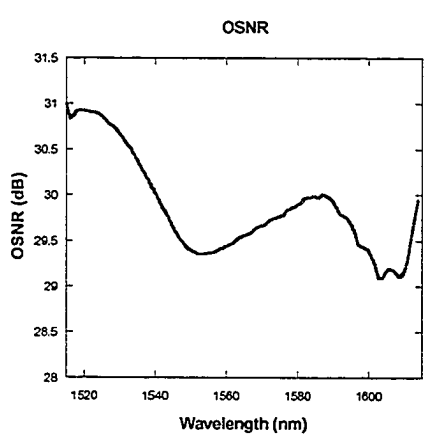

Figure 5.3 (a) OSNR flatness result using one pump in the forward pumping scheme;

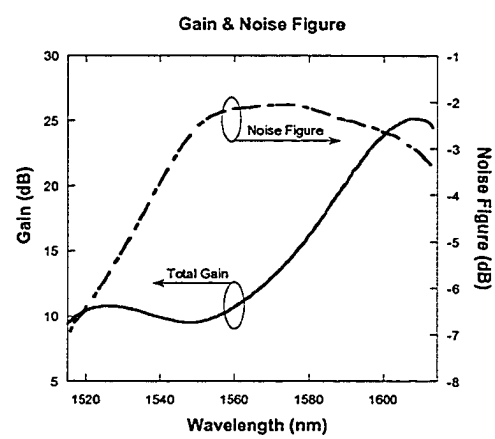

(b) Corresponding gain and noise figure

5.2.2 Two pumps

Figure 5.4 (a) shows the OSNR flatness result with two incoherent forward pumps. The parameters used in the simulation are listed in Table 5.2. Figure 5.4 (b) shows the average gain and noise figure level result in the simulation. The ripple of OSNR is less than 0.6 dB, which is a big improvement compared to using one pump. The ripple of the total gain is about 8 dB, which is very large for the real application.

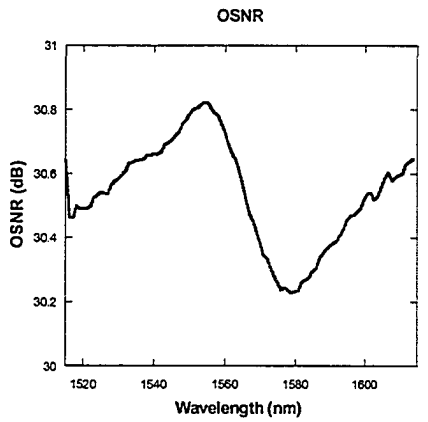

Figure 5.4 (a) OSNR flatness result using one pump in the forward pumping scheme;

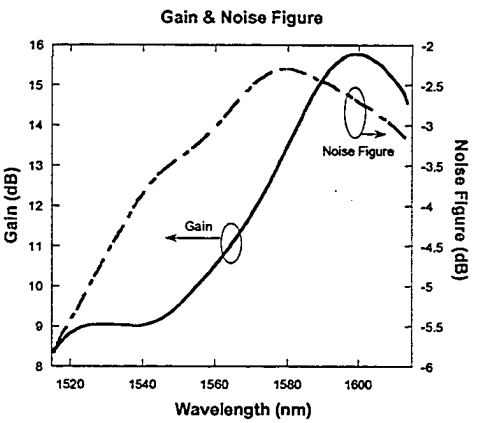

(b) Corresponding gain and noise figure

		Center Wavelength (nm)	FWHM (nm)	Total Pump Power (mW)
Pump for TW-Reach	Pump1	1400	28	536
	Pump2	1447	15	
Pump for DCF	Pump1	1484	12	400
	Pump2	1506	10	

Table 5.2 Parameters used in the forward pumping simulation with two incoherent pumps

A reversed result can be observed in the forward pumping regime: OSNR takes its highest value at the shortest wavelengths and drops down at longer wavelength. This is because at a high frequency window there is more power transferred from pump to signal, the signal power experiences more gain than ASE power; this is the reason why at low wavelength side, the OSNR is higher. In the

simulation, methods were used to adjust the power at the longer wavelength to flatten the overall OSNR value, according to this theoretical reasoning. This phenomenon will also be used in *Chapter 6.*

5.3 Summary

For pursuing the OSNR flatness, two pumping schemes were employed: backward pumping and forward pumping. OSNR from noise due to Double Rayleigh Scattering is around 30 dB for both pumping configurations.

With an average gain level of about 10 dB, the OSNR flatness of the dispersion compensated Raman amplifier was obtained within 100 nm bandwidth (from 1515 to 1615 nm), covering C-band, L-band and S-band, without band splitting.

To conclude this chapter: simulations on OSNR flatness were presented. In backward pumping scheme, with one incoherent pump, the OSNR ripple of 1.5 dB was obtained, with the average OSNR level of 29.5 dB; with two incoherent pumps, OSNR ripple of 0.8 dB was achieved, with the average OSNR level of 28.2 dB. In the forward pumping scheme, with one incoherent pump, the OSNR ripple was 2 dB with average level of 29.5 dB; with two incoherent pumps, the OSNR ripple was 0.6 dB with average level of 30.6 dB. But good OSNR flatness was achieved yielding a big gain ripple.

Because of the trade-off between gain and OSNR flatness, in the next chapter, we will focus on pursuing the flatness of both gain and OSNR simultaneously.

Chapter 6

Trade-off of flat gain and flat OSNR

In the design of higher capacity and longer distance WDM transmission systems, it is very critical to make all the signal channels having almost equal performances in terms of signal power, OSNR, noise figure and so on. Both signal-to-signal stimulated Raman scattering and wavelength dependence of the fiber loss degrade the signal power and the OSNR, especially in shorter wavelength band. In order to compensate for these degradations, it is useful to independently control the spectra of Raman gain and OSNR. However, from the results of *Chapter 4* and *Chapter 5*, we can see that there is always a trade-off between Gain flatness and OSNR flatness. If the Gain tilt is made flatter, the OSNR tilt is seen bigger, and vice versa. Then the question arises: can we have the Gain and OSNR flatness simultaneously in order to achieve a better system performance? In this chapter, first, clear comparison will be illustrated in order to see the relations between gain and OSNR flatness. Then, investigations will be done theoretically to find the methods for pursuing a better transmission performance with bidirectional pumping scheme. Last, simulation results will be shown based on this analysis. We will see from the simulations that using a bidirectional pumping method, a better gain and OSNR flatness can be obtained; and the overall transmission system performance can be improved consequently.

6.1 Gain and OSNR flatness comparison

Figure 6.1 gives the results of the two pumps backward pumping simulations done in *Chapter 4* and *Chapter 5*; the gain and OSNR were put together in one chart for a better flatness comparison. From the figure, we can see that with two pumps backward pumping, gain ripple of 0.8 dB was obtained, and the corresponding OSNR ripple was 1.2 dB. When an adjustment was made to achieve an OSNR ripple of 0.8 dB, gain ripple became as much as 7.5 dB. It was a great sacrifice.

Figure 6.2 gives the results of the two pumps forward pumping simulations done in *Chapter 4* and *Chapter 5*. We can see that when the gain ripple was made to be 0.8 dB, the ripple of OSNR was 2.5 dB. After the OSNR ripple was adjusted to be 0.6 dB, the gain tilt was seen to be 7.5 dB, same as the result in the backward pumping case. The bargain of the flatness between gain and OSNR can be seen clearly.

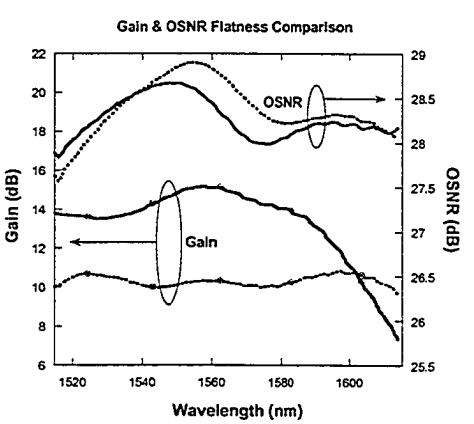

Figure 6.1 Gain & OSNR flatness comparison result from two pumps **backward** pumping. The dashed lines are gain flatness. The solid lines are OSNR flatness.

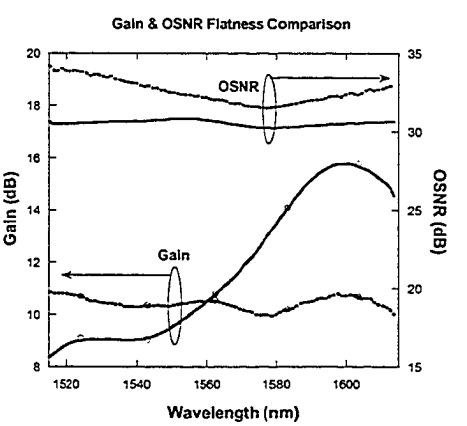

Figure 6.2 Gain & OSNR flatness comparison result from two pumps **forward** pumping. The dashed lines are gain flatness. The solid lines are OSNR flatness.

6.2 Theoretical analysis

From the figures above and former chapters, we can see that the backward pumping OSNR takes the lowest value at the shortest wavelength channels; whilst the forward pumping OSNR is highest at the shortest wavelength channels, and drops down gradually. This is because in the backward pumping scheme, stimulated Raman scattering between the signals causes power to be transferred from the shortest to longest wavelength channels. Therefore, the shortest wavelengths experience additional loss. Also, the same interaction between the pumps reduces the penetration depth for the shortest wavelength pumps, further degrading the span noise performance at short signal wavelengths. The longest wavelength pumps, on the other hand, are amplified and so penetrate deeper into the span, improving the OSNR for the longest wavelength channels. In addition, the close spectra proximity of the longest wavelength pumps to the shortest wavelength signals increases ASE generation in this spectral region because of its inherent temperature dependence [3]. All these effects lead to an OSNR tilt across the signal band with the worst OSNR at shortest wavelengths and the best at longest [3].

In the forward pumping scheme, the signals and pumps are traveling in the same direction. A type of parametric interaction between pumps and signals will cause more noise and degrade the OSNR, and this interaction is stronger at longer wavelengths [21]. Moreover, extra power transferred to longer wavelengths tends to

cause more Four Wave Mixing (FWM) and other nonlinearities, which contributes to the degradation of OSNR at longer wavelength channels [7] ~ [11].

The *New Design Method*[16] mentioned in the former chapters improves the noise performance by moving part of the gain from distributed Raman amplifier to discrete module, in turn, less power transfer at the long wavelengths side causes the dropping of OSNR in this region. This method is for purely backward pumping scheme. The drawback of this method is that the poor OSNR is not improved at the short wavelengths, although OSNR flatness can be achieved.

Another proposal to compensate the OSNR tilt is to preferentially forward pump the shortest wavelength channels [7]. Figure 6.3 shows measurement results that demonstrate the benefits of this approach. Here two forward pumps were added at the short wavelength channels. The forward gain they provided lifted OSNR of the short wavelengths. This approach was done on the distributed Raman amplification systems.

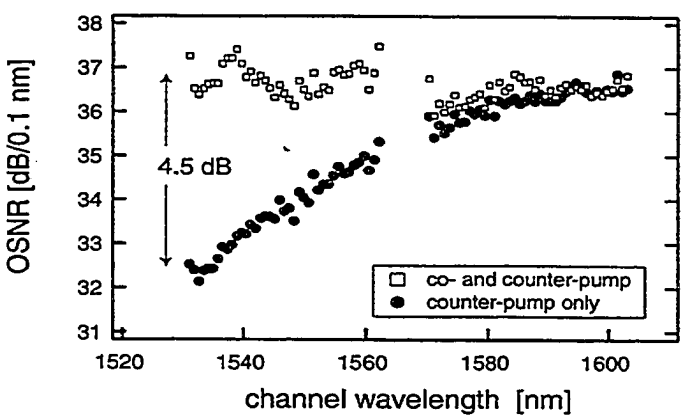

Fig. 6.3 OSNR tilt correction in C- and L-band system by preferentially forward pumping the short wavelength channels. Ref.[3]

In this thesis, the dispersion compensating fiber as a discrete Raman amplifier is used in addition to distributed Raman amplifier. Under this condition, a

combination of those two methods will be used, taking the advantages of the *New Design Method* and forward pumping short wavelength in the backward pumping scheme. Simulations will be done with bidirectional pumping with a slight adjustment of the pumping power to forward and backward pump, to pursue a better gain and OSNR flatness, so to have a better system noise performance.

6.3 Gain & OSNR flatness of FRA's with bidirectional pumping

Figure 6.4 illustrates the simulation setup of the bidirectional pumping dispersion compensation Raman amplifier. In order to improve the noise characteristics and flatten the OSNR, both transmission fiber and DCF are pumped with first-order forward pumping and backward pumping simultaneously, forming a bidirectional pumping regime.

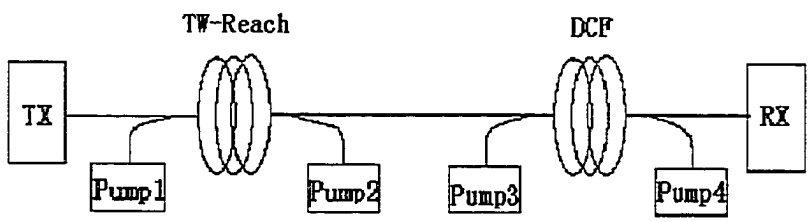

Figure 6.4 Schematic of bidirectional pumping scheme

Figure 6.5 gives the total gain output results using bidirectional pumping. And Figure 6.6 shows the corresponding noise figure and OSNR outputs from distributed Raman amplifier and its discrete counterpart. Both total gain and OSNR flatness are obtained with the ripples less than 1 dB within 100 nm bandwidth from 1515 to 1615 nm. The parameters used in this simulation are listed in Table 6.1. Compared to the simulation results from *Chapter 4* and *Chapter 5*, we can see that with the same gain

level, bidirectional pumping has a better OSNR than purely forward and backward pumping scheme. Using discrete module causes OSNR degradation of 2.5 dB (from 35.5 to 33 dB), but the result is still better than either forward pumping or backward pumping.

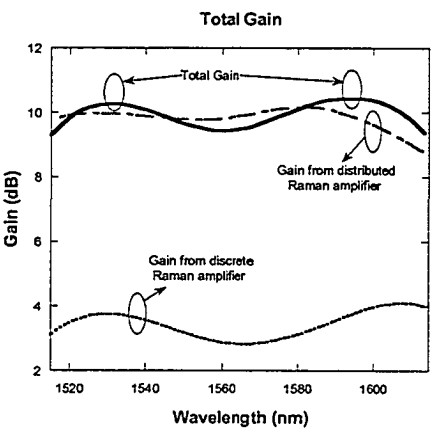

Figure 6.5 Total gain output from the bidirectional pumping scheme

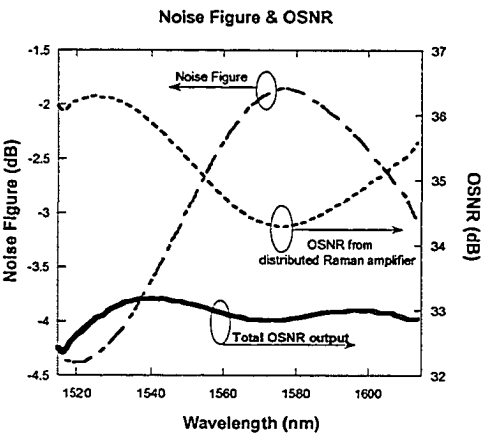

Figure 6.6 Corresponding noise figure & OSNR outputs

		Center Wavelength (nm)	FWHM (nm)	Power (mW)
TW-Reach	Backward pump	1480	35	200
	Forward pump	1410	28	475
DCF	Backward pump	1430	20	90
	Forward pump	1504	20	90

Table 6.1 Parameters used in the bidirectional pumping

The reason why the gain from the distributed Raman amplifier is very close to the total gain output is that in the DCF as a discrete Raman amplifier, all of the pump powers are confined to the lumped elements. If the pump power is comparative to DRA, more DRS noise will be created due to the high double Rayleigh scattering coefficient in the DCF, so the noise performance drops sharply especially at the long

wavelength side when the pump power exceeds a certain level. For the purpose of achieving OSNR flatness at the longest wavelengths, the pump power was kept to a small level (90 mW) for both forward and backward pump. Thus, the distributed Raman amplifier contributes a large portion of the gain, only leaves a gain tilt at the longest wavelengths. In the discrete module, forward pump is used to push up the OSNR tilt at the shortest wavelengths; while backward pump is to pull down the OSNR at the longest wavelengths, and compensates the gain tilt in this area at the same time.

6.4 Summary

This chapter has investigated the approaches of pursuing both gain and OSNR flatness simultaneously on the dual-stage fiber Raman amplification module, namely a distributed Raman amplifier followed by a DCF as the discrete Raman amplifier, for the purpose of having a more steady system output performance. Based on the analysis of the results from *Chapter 4* and *Chapter 5*, the treatment was to use the combination of *New Design Method* and bidirectional pumping scheme to reduce the gain and OSNR ripple.

The simulations were performed and the results were shown. The ripples of both total gain and OSNR output were adjusted to be less than 1 dB, which is considered to be "very small". Although a smaller ripple than this can possibly be obtained, with further adjustment and optimizing the pump power, center wavelength or FWHM, the main point here is to introduce and verify our proposal.

Bidirectional pumping with pump laser RINs less than –140dB/Hz has allowed an average OSNR improvement by 6 dB in the transmission fiber--the first stage, compared to either backward pumping or forward pumping alone. Even for the second stage--after the discrete Raman amplifier, the OSNR was still higher than those two schemes. This highlights the prospect of possible performance enhancement in high bit rate multiple long-span WDM systems by bidirectionally pumped dispersion compensating Raman amplification, as compared to backward pumping only, or unrepeated transmissions with adoption of fiber effective area management and remote pumping.

Note that with low to medium pump powers (<~2W), bidirectional pumping provides the optimum performance in terms of gain and OSNR degradation. But for high pump powers (>~2W), a backward propagating pump performs better, as the gain and OSNR are degraded in the other two configurations by higher order Stokes generation [22].

The main conclusions for this chapter are:

1. Both gain and OSNR flatness can be achieved using the combination of *New Design Method* and bidirectional pumping by the right power adjustment on distributed and discrete Raman amplification modules.

2. Although the DCF as the discrete Raman amplification can cause OSNR degradation from the distributed counterpart, the OSNR is still better than purely forward or backward pumping the dual-stage Raman amplification.

Also from the results of this chapter, we can conclude that DCF not only can

be used as discrete Raman amplifier to improve gain and compensate the loss from the distributed Raman amplifier; with a suitable design and application, it also helps to achieve a flatter Gain and OSNR for the broadband WDM system.

Chapter 7

Conclusion

This thesis has investigated the noise performance of a dispersion compensating fiber Raman amplifier module by employing a novel incoherent pump source. The comparison between using coherent and incoherent pumps was done and the performance improvement was given. Gain and OSNR flatness through 100 nm bandwidth covering *S*-, *C*- and *L*-band were achieved simultaneously.

First, a general Raman amplifier model was presented. It includes the Stokes and anti-Stokes emission, Rayleigh scattering and the temperature dependence of the emission spectrum—these are very important effects for accurate modeling of practical Raman amplifiers. The correctness of this modeling was also verified. The simulations were done using the same setup and parameters with the example in which the original model was given.

An incoherent pump source and its modeling were introduced. Simulations using coherent pumps on the dual-stage Raman amplifier—distributed Raman amplifier followed by a DCF as the discrete Raman amplifier were done. The purpose of doing this is, firstly, to introduce a *New Design Method* presented in [16] to improve the system noise performance of DCRA; secondly, to give an example of gain and OSNR flatness that can be achieved using coherent pump lasers. Moreover,

it is to have a point of reference for better comparison in the following chapters.

Gain and OSNR flatness within 100 nm bandwidth for DCRA were obtained employing incoherent pumps by adoption of the *New Design Method* in *Chapter 4* and *Chapter 5*, respectively. Through the two chapters, a trade-off relation can be seen: pursuing gain flatness, OSNR flatness has to be sacrificed, and vice versa. Another two conclusions are: 1: using one incoherent pump can have the same gain ripple as using six coherent pumps in the two-stage DCRA within 100 nm bandwidth; 2: using the incoherent pump with low RIN, forward pumping scheme can have a better OSNR than backward pumping, especially at the short wavelength side.

Simulations on pursuing gain and OSNR flatness simultaneously were done. The results show that with employing the combination of *New Design Method* and bidirectional pumping regime, simultaneous gain and OSNR flatness can be achieved within 100 nm in DCRA module, and the system output stability and noise performance were improved.

It needs to be noted that, theoretically, the more pumps used in the amplification system, the better performance it will have; surely the flatter gain and OSNR can be obtained, no matter for coherent or incoherent pumps. However, using more pumps can cause application complexity and high cost, and sometimes it may reduce the whole system performance. So, to obtain an acceptable flatness level, the less pumps, the better.

References

[1] L. Mollenauer, J. Gordon, M. Islam, "Soliton propagation in long fibers with periodically compensated loss," *IEEE J. Quantum Electron., vol. QE-22, pp. 157-173, 1986.*

[2] M. Islam, "Raman amplifiers for telecommunications," *IEEE J. Selected Topics in Quantum Electron. vol.8, pp.548-559, 2002.*

[3] J. Bromage, "Raman amplification for fiber communication systems", *J. Lightwave Tech., vol.22, pp. 79-93, 2004.*

[4] V. Perlin, G. Winful, "Optimal design of flat gain wide band fiber Raman amplifiers," *J. Lightwave Tech., vol.20, pp.250-254, 2002.*

[5] V. Perlin, G. Winful, "On distributed Raman amplification for ultrabroad-band long-haul WDM systems," *J. Lightwave Tech., vol.20, pp.409-416, 2002.*

[6] X. Liu, B. Lee, "Optimal design for ultra-broad band amplifiers," *J. Lightwave Tech., vol.21, pp.3446-3455, 2003.*

[7] T. Kung, C. Chang, J. Dung, S. Chi, "Four-wave mixing between pump and signal in a distributed Raman amplfier," *J. Lightwave Tech., vol.21, pp.1164-1170, 2003.*

[8] J. Bouteiller, L. Leng, C. Headley, "Pump–pump four-wave mixing in distributed Raman amplified systems," *J. Lightwave Tech., vol.22, pp.723-732, 2004"*

[9] W. Wong, C. Chen, M. Ho, H. Lee, "Phase-matched four-wave mixing between pumps and signals in a forward-pumped Raman amplifier," *IEEE Photon. Tech. Lett., vol.15, pp.209-211, 2003.*

[10] X. Zhou, M. Birk, S. Woodward, "Pump-noise induced FWM effect and its reduction in a distributed Raman fiber amplifiers," *IEEE Photon. Tech. Lett., vol.14, pp.1686-1688, 2002.*

[11] F. Pasquale F. Meli, "New Raman pump module for reducing pump–signal four-wave-mixing interaction in forward-pumped distributed Raman amplifiers," *J. Lightwave Tech., vol.22, pp.1742-1748, 2003*

[12] S. Sugliani, G. Sacchi, G. Bolognini, S. Faralli, F. Pasquale, "Effective suppression of penalties induced by parametric nonlinear interaction in distributed Raman amplifiers based on NZ-DS fibers," *IEEE Photon. Tech. Lett., vol.16, pp.81-83, 2004.*

[13] G. Bolognini, S. Sugliani, F. Pasquale, "Double Rayleigh scattering noise in Raman amplifiers using pump time-division-multiplexing schemes," *IEEE Photon. Tech. Lett., vol.16, pp.1286-1288, 2004.*

[14] J. Bromage, P. Winzer, L. Nelson, M. Mermelstein, C. Headley, "Amplified spontaneous emission in pulse-pumped Raman amplifiers," *IEEE Photon. Tech. Lett., vol.15, pp.667-669, 2003.*

[15] D. Vakhshoori, M. Azimi, P. Chen, B. Han, M. Jiang, L. Knopp, C. Lu, Y. Shen, G. Rodes, S. Vote, P. Wang, X. Zhu, "Raman amplification using high-power incoherent semiconductor pump sources", *OFC 2003, Paper PD47.*

[16] X. Zhou, M. Birk, "New design method for a WDM system employing broad-band Raman amplification", *IEEE Photon. Tech. Lett., vol.16, pp.912-914, 2004.*

[17] S. Kado, Y. Emori, S. Namiki, "Gain and noise tilt control in multi-wavelength bi-directionally pumped Raman amplifier," *OFC 2002, pp.62-63, Paper TuJ4.*

[18] I. Mandelbaum, M. Bolshtyansky, "Raman amplifier model in single-mode optical fiber", *IEEE Photon. Tech. Lett., vol.15, pp. 1704-1706, 2003.*

[19] X. Liu, B. Lee, "A fast and stable method for Raman amplifier propagation equations", *Optics Express vol.11, pp.2163- 2176, 2003.*

[20] K. Rottwitt, A. Stentz, L. Leng, M. Lines, H. Smith, "Scaling of the Raman gain coefficient: applications to Germanosilicate fibers", *IEEE J. Lightwave Technol., vol.21, pp. 1652-1662, 2003.*

[21] M.C Ho, W.S Wong, "Parametric interactions between pumps and signals in a forward-pumped Raman amplifier". *CLEO '02. Technical Digest. Summaries of Papers Presented on 19-24 May 2002.*

[22] E.A Kunarajah, J.J Lepley, A.S Siddiqui, "An accurate numerical model for distributed Raman amplifiers" *Optical Communication, 2001. ECOC '01. 27th European Conference on , Volume: 2 , 30 Sept.-4 Oct. 2001*

[23] *http://www.ahuracorp.com/v6/index_3_04.html at Feb.21 2004.*

[24] Y. Emori. "100nm bandwidth flat gain Raman amplifiers pumped and gain-equalized by 12-wavelength-channel WDM high power laser diodes" *OFC/IOOC '99. Technical Digest, Vol. Supplement, 21-26 Feb. 1999.*

[25] M. Nissov, K. Rottwitt, H.D. Kidorf, M.X. Ma, "Rayleigh crosstalk in long cascades of distributed unsaturated Raman amplifiers," *Electronics Letter, vol.35, pp.997-998,1999.*

[26] G. Agrawal "Fiber-Optic Communication Systems: Evolution of Lightwave Systems," *Chapter 1, NY, third edition, 2002.*

[27] Y. Yamamoto, "Characteristics of AlGaAs Fabry-Perot cavity type laser amplifiers," *IEEE Journal of Quantum Electronics, QE-16(10), pp.1047-1052, 1980.*

[28] T. Saitoh T. Mukai, "1.5-um GaInAs traveling-wave semiconductor laser amplifier," *IEEE Journal of Quantum Electronics, QE-23(6, pp.1010-1020, 1987.*

[29] P. Kuindersma, G. Cuijpers, J. Reid, G. Hoven, and S. Walczyk, "An experimental analysis of the system performance of cascades of 1.3 um semiconductor optical amplifiers," *European Conference on Optical Communication in Edinbourgh, United Kingdom, September, 1997, pp. 79-82.*

[30] R. Laming, M. Zervas, D. Payne, "54 dB gain quantum-noise-limited Erbium-doped fiber amplifier," *European Conference on Optical Communication in Berlin, Germany, vol. 1, pp. 89-92, 1992.*

[31] R. Stolen, E. Ippen, "Raman gain in glass optical waveguides," *Appl. Phys. Lett., vol.22, page 276-278, 1973.*

[32] G. Agrawal, "Fiber-optic communication systems: amplifier performance," *The Institute of Optics University of Rochester, Rochester, NY, third edition, 2002.*

[33] J. Bouteiller, K. Brar, S. Radic, J. Bromage, Z. Wang, C. Headley, "Dual-order Raman pump providing improved noise figure and large gain bandwidth," *OFC 2002, post deadline Feb.3.*

[34] K. Rottwitt, A. Stentz, T. Nielsen, P. Hansen, K. Feder, K. Walker, "Transparent

80 km bi-directionally pumped distributed Raman amplifier with second-order pumping," *ECOC 1999, vol.2 pp.144-145.*

[35] J. Nicholson, J. Fini, J. Bouteiller, J. Bromage, K. Brar, "Stretched ultrashort pulses for high repetition rate swept wavelength Raman pumping," *J. Lightwave Tech., vol.22, pp.71-78, 2004.*

[36] C. Raman K. Krishnan, "A new type of secondary radiation," *Nature, vol.121 , pp.501, 1928.*

[37] R. Stolen, "Nonlinear properties of optical fibers," *Optical fiber Telecommunications, Chapter 5, pp.127-133. Academic Press, New York, 1979.*

[38] G. Agrawal, "Nonlinear Fiber Optics," *Chapter 8, pp.316-336. Academic Press, San Diego, second edition, 1995.*

[39] G. Agrawal, "Fiber-optic communication systems: Raman amplifiers," *Chapter 6, pp.243. The Institute of Optics University of Rochester, Rochester, NY, third edition, 2002.*

[40] A. Chraplyvy, "Optical power limits in multi-channel wavelength-division multiplexed systems due to stimulated Raman scattering," *Electron. Letter, vol.20, pp. 58-59, 1984.*

[41] M. Nissov, "Long-Haul Optical Transmission Using Distributed Raman Amplification," *Chapter 3, pp.42-45, December, 1997.*

[42] R. Stolen, "Polarization effects in fiber Raman and Brillouin lasers," *IEEE, Journal Quantum Electron., vol.Qe-15, pp.1157-1160, 1979.*

[43] R. Stolen, C. Lee, R. Jain, "Development of the stimulated Raman spectrum in

single-mode silica fibers," *J. Opt. Soc. Amer. B, vol.1, pp.652-657, 1984.*

[44] H. Kidorf, K. Rottwitt, M. Nissov, M. Ma, E. Rabarijaona, "Pump interactions in a 100-nm bandwidth Raman amplifier," *IEEE Photon. Technol. Letters, vol.11, pp.530-532, May 1999.*

[45] M. Achtenhagen, T. Chang, B. Nyman, A. Hardy, "Analysis of a multiple-pump Raman amplifier," *Appl. Phys. Lett., vol.78, pp.1322-1324, 2001.*

[46] A. Berntson, S. Popov, E. Vanin, G Jacobsen, J. Karlsson, "Polarization dependence and gain tilt of Raman amplifiers for WDM systems," *OFC 2001, Baltimore, MD, Paper MI2-1.*

[47] B. Pedersen, A. Bjarklev, J. Povlsen, K. Dybdal, C. Larsen, "The design of Erbium-doped fiber amplifers," *Journal Lightwave Technology, vol.9 pp.1105-1112, September 1991.*

[48] http://www.ofsoptics.com.

[49] S.A.E.Lewis, F. Koch, S.V. Chernikov, J.R. Taylor, , "Low-noise high gain dispersion compensating broadband Raman amplifier" *Optical Fiber Communication Conference, 2000 , Volume: 1 , 7-10 March 2000 Pp.5 - 7 vol.1*

[50] P. Shirley, M.N.C. Freitas, R.T.R. Almeida, L.C. Calmon, "Raman Amplifier Performance of Dispersion Compensating Fibers" *Microwave and Optoelectronics Conference, 2003. IMOC 2003. Proceedings of the 2003 SBMO/IEEE MTT-S International , Volume: 2 , 20-23 Sept. 2003 pp.553 – 558 vol.2*

[51] A. Kimsas, P. Staubo, S. Bjornstad, B. Slagsvold, A. Sudbo, "A dispersion

compensating Raman amplifier with reduced double Rayleigh backscattering, employing standard DCF" *Proceedings of 2004 6th International Conference on Transparent Optical Networks, 2004. Vol.2 , 4-8 July 2004 Pages:326 – 329 vol.2*

[52] J.W. Nicholson, "Dispersion compensating Raman amplifiers with pump reflectors for increased efficiency" *Journal Lightwave Technology, Volume: 21 , Issue: 8 , Aug. 2003*

Acronyms

ASE	amplified spontaneous emission
BER	bit error rate
DFRA	distributed fiber Raman amplifier
DCF	dispersion compensating fiber
DCRA	dispersion compensated Raman amplifier
DRB	double Rayleigh backscattering
EDFA	erbium-doped fiber amplifier
FRA	fiber Raman amplifier
FWHM	full-width at half-maximum
FWM	four wave mixing
MPI	multiple-path interference
OSNR	optical signal to noise ratio
RIN	relative intensity noise
SMF	single mode fiber
SBS	stimulated Brillouin scattering
SRS	stimulated Raman scattering
SPOA	seeded power optical amplifier
TDM	time division multiplexing
WDM	wavelength-division multiplexed